Contents lists available at ScienceDirect

Current Research in Food Science

Modulation of gut microbiota and markers of metabolic syndrome in mice on cholesterol and fat enriched diet by butterfly pea flower kombucha

Happy Kurnia Permatasari [a,*,2,1], Fahrul Nurkolis [b,2], William Ben Gunawan [c], Vincentius Mario Yusuf [d], Muhammad Yusuf [d], Rio Jati Kusuma [e], Nindy Sabrina [f], Farizal Rizky Muharram [g,1], Nurpudji Astuti Taslim [h,1], Nelly Mayulu [i,1], Siti Chairiyah Batubara [j], Mrinal Samtiya [k], Hardinsyah Hardinsyah [l,1], Apollinaire Tsopmo [m,1]

[a] Biochemistry and Biomolecular, Faculty of Medicine, Brawijaya University, Malang, 65145, Indonesia
[b] Biological Sciences, State Islamic University of Sunan Kalijaga (UIN Sunan Kalijaga), Yogyakarta, Yogyakarta, 55281, Indonesia
[c] Nutrition Science Department, Faculty of Medicine, Diponegoro University, Semarang, Central Java, 50275, Indonesia
[d] Medical Programme, Faculty of Medicine Universitas Brawijaya, Malang, 65145, Indonesia
[e] Department of Nutrition and Health, Faculty of Medicine, Public Health, and Nursing, Universitas Gadjah Mada, Yogyakarta, 55223, Indonesia
[f] Department of Nutrition, Dietetics, and Food, Faculty of Medicine, Nursing, and Health Sciences, Monash University, Wellington Rd, Clayton VIC 3800, Australia
[g] Medical Faculty of Airlangga University, Jl. Mayjen. Prof. Dr. Moestopo 47, Surabaya, Jawa Timur 60132, Indonesia
[h] Clinical Nutrition, Faculty of Medicine, Hasanuddin University, Makassar, 90245, Indonesia
[i] Nutrition and Food, Faculty of Medicine, Sam Ratulangi University, Manado, 95115, Indonesia
[j] Food Technology Department, Sahid University of Jakarta, South Jakarta, 12870, Indonesia
[k] Department of Nutrition Biology, Central University of Haryana, 123029, India
[l] Applied Nutrition, Faculty of Human Ecology, IPB University, Bogor, West Java, 16680, Indonesia
[m] Department of Chemistry, Carleton University, 1125 Colonel by Drive, Ottawa, K1S5B6, Canada

ARTICLE INFO

ABSTRACT

Clitoria ternatea, with an alternative name, Butterfly pea, is increasingly being explored for medical purposes and the development of a wide range of processed products. This study aimed to incorporate Butterfly pea into an innovative probiotic drink through a symbiotic culture of bacteria and yeast (SCOBY) fermentation and to evaluate the biological activity. The benefits of the drink, referred to as butterfly pea flower kombucha (KBPF) was determined in vitro and in metabolically disorder mice that receive a diet rich in cholesterol and fat (CFED). Forty white male were categorized into four groups, i.e., A = Control/Normal Diet; B = CFED alone; C = CFED + KBPF 65 mg/kg BW (Body Weight); D = CFED + KBPF 130 mg/kg BW, and then sacrificed after 6 weeks of intervention. Seventy-nine secondary metabolite compounds were successfully identified in KBPF using LC-HRMS. In vitro studies showed the potential activity of KBPF in inhibiting not only ABTS, but also lipid (lipase) and carbohydrate (α-amylase, α-glucosidase) hydrolyzing enzymes to levels similar to acarbose control at 50–250 μg/mL. In the in vivo study, the administration of KBPF (130 mg/kg BW) significantly alleviated metabolic disorders caused by high-fat diet. Specifically, lipid profile (HDL, LDL, TC, TG), blood glucose, markers of oxidative stress (SOD liver), metabolic enzymes (lipase, amylase), and markers of inflammation (PGC-1α, TNF-α, and IL-10) were in most cases restored to normal values. Additionally, the gut microbiota community analysis showed that KBPF has a positive effect (p = 0.01) on both the Bacteroidetes phylum and the Firmicutes phylum. The new KBPF drink is a promising therapeutic functional food for preventing metabolic diseases.

* Corresponding author.
E-mail address: happykp@ub.ac.id (H.K. Permatasari).
[1] Considered as senior authors.
[2] These authors provide equal contribution to this work.

Abbreviations used

ABTS	2,2'-Azino-bis(3-ethylbenzothiazoline-6-sulfonic acid) or diammonium salt radical cation
AOAC	Association of Official Analytical Chemists
ARRIVE	Animal Research: Reporting of In Vivo Experiments
CFED	cholesterol- and fat-enriched diet
CIOMS	Council of International Organizations of Medical Sciences
DMSO	dimethyl sulfoxide
FER	Food Efficiency Ratio
HDL	high-density lipoprotein
HPLC	high-performance liquid chromatography
IL-10	Interleukin 10
KBPF	kombucha butterfly pea flower

LC-HRMS	Liquid Chromatography High-Resolution Mass Spectrometry
LDL	low-density lipoprotein
LEfSe	Linear discriminant analysis Effect Size;
MetS	Metabolic Syndrome
OTUs	operational taxonomic units
PGC-1α	Peroxisome proliferator-activated receptor-γ coactivator 1-α
SCOBY	symbiotic culture of bacteria and yeast
SOD	superoxide dismutase
TG	Triglyceride
TNF	Tumor necrosis factor
Trolox	6-Hydroxy-2,5,7,8-tetramethylchroman-2-carboxylic acid

---

1. Introduction

Metabolic condition or syndrome (MetS) is a multifactorial disorder manifested by an accumulation of different health disorders, impaired glucose tolerance, hyperglycemia, hypertension, central obesity, and dyslipidemia (Torres et al., 2019; Noce et al., 2021). Imbalance or overload of visceral adiposity is the origin of the rising of the pro-inflammatory adipokine (tumor necrosis factor, TNF), which contributes to the ubiquity of chronic inflammatory characteristics of low degrees MetS (Torres et al., 2019). Subsequent increases of adipose tissue of the stomach can cause systemic inflammation, followed by oxidative stress, endothelial damage, and insulin resistance. This dysfunction, which occurs in conjunction with other metabolic disorders, may further lead to vascular disease, non-alcoholic fatty liver disease, obesity, type 2 diabetes, and possibly premature mortality (Torres et al., 2019; Chen et al., 2021). MetS itself is influenced for example by genetic inheritance, day-to-day lifestyle (i.e., diet, inactivity, smoking), insufficient or sleep disturbances, and chronic stress, which then contribute to the imbalance of various metabolic processes and their associated disease conditions (Saklayen, 2018; Hardy et al., 2021). The rapid progression of MetS has made it an important public health problem globally (Noce et al., 2021; Saklayen, 2018; Rojas et al., 2021).

The primary clinical practice guidelines in MetS cases focuses on an initial request to change lifestyle and retrict calorie (Grundy, 2016). Lifestyle interventions are recognized to be potentially effective in preventing the occurrence of MetS and alleviating the symptom of metabolic disorders (van Namen et al., 2019). In this regard, systematic reviews and recent meta-analyses have shown that supervised multidimensional lifestyle modifications, including coupling physical activity with diet, can control MetS and its clinical symptoms (van Namen et al., 2019). Nonetheless, MetS patients require pharmaceuticals support, several of which cause adverse effects, whereas natural bioactive compounds with antioxidant, immune system modulation, and enzyme regulation properties may be a safer alternative (Torres et al., 2020). The bioactive natural molecules and functionalized foods have then emerged as an alternative therapy for the management of MetS. The rational lies in their capacity to restore for example, the redox balance, gut microbiota balance, intestinal barrier function, energy homeostasis (improving lipid profile and PGC-1α), and modulate the immune system (Noce et al., 2021; Torres et al., 2020).

Clitoria ternatea or Butterfly pea is a perennial herb of the plant family *Fabaceae*. The species is an alternative medicine for various ailments and possess secondary metabolites with antioxidant activities which make it interested in food formulation (Oguis et al., 2019). This study aims to incorporate Butterfly pea into a new probiotic drink or Kombucha using the symbiotic culture of bacteria and yeast (SCOBY) fermentation methods. This new drink is expected to be in line with the theory, which states that fermentation can increase the bioactive properties of a food ingredient. The study further evaluates the benefits of the kombucha butterfly pea flower (KBPF) drink on the immune system modulation and markers of metabolic disorders through in vitro approach and mice fed on a cholesterol- and fat-enriched diet (CFED).

2. Materials and methods

2.1. Collection dan preparation of butterfly pea flower ingredients (Clitoria ternatea)

Butterfly pea flower (*Clitoria ternatea*; Taxonomic Serial No.: 26543) was collected from Yogyakarta, Indonesia (Wirokerten, Banguntapan, Bantul Regency, Google Maps Coordinates = −7.8484152, 110.3993969). The identification and authentication of botanical species was done at the Biology Department, State Islamic University of Sunan Kalijaga, Special Region of Yogyakarta, Indonesia. Specimens were collected for feature reference. Butterfly pea flowers (*C. ternatea*) double petals were cleaned and then dried using a drying oven Uf 55 at a temperature of 50 °C for 4 h, referring to Martini et al., 2020 (Martini et al., 2020); resulting in dried butterfly pea flowers with a moisture content of 10% (referring to the AOAC methods protocol).

2.2. Kombucha butterfly pea flower (KBPF) drink formulation

The ingredients of the kombucha butterfly pea flower (KBPF) drink formula consist of 2,000 mL of water, 24 g of dehydrated butterfly pea flowers, 300 g of granulated sugar (sugar cane), 10 g of SCOBY gel, and 166 g v/v of SCOBY starter solution, making the overall total to 2,500 mL (2.5 L). Two liters of water were heated (about 50–80 °C), then 300 g of granulated sugar cane were added, stirred until dissolved, followed by 24 g of dried butterfly pea flowers. Afterward, water stirred until the color turned deep blue, turned off the stove fire, covered the pan, and left to cool. The solution was then put in a 3 L sterile bottle, and added with 10 g of SCOBY gel and 166 g v/v of SCOBY starter solution. The bottle was covered with clean gauze and tied so that the cloth closes tightly; then, it was stored in anaerobic conditions at 20–25 °C for 12 days. The formulation was designed by Dr. Siti Chairiyah Batubara, S.T. P., M.Si (Food Technology Expert Certified, Department of Food Technology, Sahid University Jakarta), taking into account previous research formulations (Permatasari et al., 2021, 2022a; Augusta et al., 2021; Tanner et al., 2022). After 12 days of fermentation, all sample drinks were stored at a refrigerator temperature of 4–8 °C for in vitro and in vivo analysis.

2.3. Metabolomic profiling untargeted

Testing services at Laboratorium Sentral Ilmu Hayati (LSIH; ISO

9001:2008 and ISO 17025:2005; Central Laboratory of Life Sciences; Brawijaya University, Malang-65145, Indonesia) were used to analyze the untargeted metabolomics profiling test on KBPF using a high performance liquid chromatography system combined with a high-resolution mass spectrometer (LC-HRMS), with the test number 040/LSIH-UB/LK/IV/2022.A volume of 50 µl of KBPF diluted 30 times with ethanol (96%) was vortexed (2,000 rpm, 2 min) continued with centrifugation at 6,000 rpm for 2 min. Supernatants were collected and then filtered using 0.22 µm syringe filters before analysis The LC-HRMS system consisted of Thermo Scientific Dionex Ultimate 3000 RSLC Nano High-Performance Liquid Chromatography (HPLC) coupled with a micro flow meter. Solvents A and B consisted of 0.1% formic acid dissolved in water and 0.1% formic acid dissolved in acetonitrile while the analytical column was Hypersil GOLD aQ 50 × 1 mm x 1.9 µ particle size which was maintained at 30 °C. Then, it was separated at a flow rate of 40 µL/min with a linear gradient over 30 min. HRMS uses Thermo Scientific Q Exactive with a full scan at 70,000 resolution, data-dependent MS2 at 17,500 resolution, and operation time duration of 30 min in both positive and negative modes.

2.4. In vitro studies

2.4.1. Lipase inhibition assay

The first step involved the solubilization of crude porcine pancreatic lipase (PPL, 1 mg/mL) in phosphate buffer (50 mM, pH 7) followed by centrifugation at 12,000g to remove insoluble materials. Enzyme stock (0.1 mg/mL) was made by a 10-times dilution of the supernation with buffer.

The lipase inhibition potential was evaluated according to the research of Permatasari et al., (2022) (Permatasari et al., 2022a). One hundred microliter of KBPF at 50, 100, 150, 200, and 250 µg/mL was mixed with 20 µL p-nitrophenyl butyrate (pNPB) 10 mM in the reaction buffer in a transparent 96-well microplate and incubated for 10 min at 37 °C. The result was compared with the reference compound orlistat (positive control), a known PPL inhibitor while the negative control was DMSO (both with and without inhibitors). Measurements were obtained with a microplate reader at 405 nm. The yield from the reaction rate of 1 µmol p-nitrophenol per minute at 37 °C was used to determine the unit of activity. The percentage of the reduction of PPL activity when incubated in the test mixture was used to determine lipase inhibition activity. Every sample was rechecked three times (triplicates) to guarantee the validity of the study results. The equation below was used to obtain the inhibitory data.

$$Inhibition\ of\ lipase\ activity = 100 - \frac{(B - Bc)}{(A - Ac)}\ x\ 100\%$$

A = Activity without inhibitor; Ac = negative control without inhibitor; B = activity with inhibitor; Bc = negative control with inhibitor.

2.4.2. α-Glucosidase inhibition assay (%)

The α-glucosidase inhibitory potential was evaluated according to a method from the literature (RodriguesMargaret et al., 1997). An amount of the enzyme, 1 mg (76 UI) was mixed with 50 mL phosphate buffer (pH 6.9) to obtain a concentration of 1.52 UI/mL which was stored at −20 °C. Then, KBPF (0.1 mL) 50, 100, 150, 200, and 250 µg/mL was combined with 0.35 ml of sucrose (65 mM) and maltose solution (65 mM), sequentially. Preheating was done (37 °C) for 5 min before adding α-glucosidase solution (0.2 mL) into the system, then kept at 37 °C for 15 min. The system was warmed up for 2 min in a water bath of 100 °C temperature. This study used acarbose as the positive control with the same treatment as KBPF. The α-glucosidase inhibitory test solution was then mixed with testing solution (0.2 mL), and color reagent (3 mL) consecutively. Next, the system was warmed up (37 °C) for 5 min, and solution absorption was examined at 505 nm afterward. The inhibitory activity was indicated by the level of glucose release during the reaction.

2.4.3. α-Amylase inhibition assay

Incubation of diluted KBPF (50, 100, 150, 200, and 250 g/mL) with sodium phosphate buffer (500 L of 0.02 M), pH 6.9 with 0.006 M NaCl, and 0.5 mg/mL porcine pancreatic α-amylase took place for 10 min at 25 °C (effective concentration 3.2.1.1). Then, to every mix was added 1% starch solution (500 µL) in assay buffer. After that, incubation at 25 °C was done for 10 min and finished with an addition of 3,5-Dinitrosalicylic (1.0 mL). The test continued with incubation in a 100 °C water bath for 5 min and then allowed to cool to 22 °C (i.e. room temperature). To record the absorbance at 540 nm, dilution with distilled water (10 mL) was perfomed to bring the readings in the acceptable range. This study used acarbose as the positive control. The reference sample includes enzymes and reagents, excluding the sample. KBPF inhibitory values were calculated according to Permatasari et al. (2022b).

2.4.4. ABTS inhibition (%) or ABTS radical scavenging activity assay

The scavenging of 2,2′-Azino-bis(3-ethylbenzothiazoline-6-sulfonic acid) or diammonium salt radical cation (ABTS+; Sigma-Aldrich) was determined based on literature procedure (Sancho et al., 2013). The 2.4 mM Potassium persulfate (2.4 mM) 7 mM ABTS (7 mM) were mixed at a ratio of 1:1, protected from light with aluminum foil, and allowed to react for 14 h at ambient temperature (22 °C) and then labelled as. The stock solution. To obtain the working solution, 1 mL of the stock solution was diluted with 60 mL of ethanol to obtain an absorbance of 0.706 at 734 nm. Fresh working solution was prepared for each test. The samples (50, 100, 150, 200, and 250 mL) were kept to react with 1 mL of ABTS working solution, and the absorbance was measured at 734 nm after 7 min. Trolox, a known antioxidant molecule was used as a positive control. All tests were performed thrice (n = 3).

$$\%\ ABTS\ radical\ scavenging\ activity = \frac{A0 - A1}{A0}\ x\ 100\%$$

A0 = absorbance of blank; A1 = absorbance of standard or sample.
The half-elimination ratio (EC$_{50}$) was used to express the radical scavenging capability of KBPF and Trolox and defined as the concentration of a sample that caused a 50% decrease in the initial radical concentration.

2.5. In vivo studies of KBPF on metabolic and inflammatory biomarker

2.5.1. Animal handling and ethical approval

Forty male albino Swiss (*Mus musculus*) mice weighing 21.53 ± 1.92 g (3–5 weeks old) were procured from Animal Model Farm Yogyakarta, Indonesia, and transported to the research location. Mice were housed in cages and kept at laboratory temperatures (27 °C) with a balanced light-dark cycle and relative humidity (50–60%). Before the experiment, all mice were acclimatized for 10 days in the laboratory. Mice had free access to normal animal feed or pellets from PT Citra Ina Feedmill and drinking water during the trial. The mice were randomly assigned into four treatment groups after a 10-day acclimatization period. The Declaration of Helsinki and the Council of International Organizations of Medical Sciences (CIOMS) are referenced in the animal use research protocol. Additionally, all steps in the animal research follow the Guidelines for Reporting In Vivo Experiments (ARRIVE) and successfully passed a review by the International Register of Preclinical Trial Protocols (PreclinicalTrials.eu) board with the registration number of PCT0000296 and Health Research and Ethics Unit of the Teaching General Hospital, Prof. Dr. RD. Kandou with approval number 101/EC/KEPK-KANDOU/VI/2022.

2.5.2. Study design of treatments

Professional vets observed the animals daily for symptoms of welfare issues (e.g., lack of appetite, ruffling, lethargy, indifference, hiding, curling up) during the trial. They are also examined every week for particular markers of health and weight reduction. The experimental group's detailed characteristics are listed in Table 1 below.

Table 1

Treatment Groups. KBPF: kombucha butterfly pea flower; CFED: cholesterol and fat-enriched diet.

Treatment Groups	Description
CON-NORM (**A; Normal Control**)	Control group without KBPF; given a standard pellet diet and ad libitum water.
CON-NEG (**B; Negative Control**)	Control group without KBPF; given a CFED and ad libitum water.
SG-L (**C; Low Dose**)	Treatment group with 65 mg/kg BW KBPF, a CFED, and ad libitum water.
SG-H (**D; High Dose**)	Treatment group with 130 mg/kg BW KBPF, a CFED, and ad libitum water.

A dose of KBPF was orally given and performed by a certified professional. During the whole experiment, the daily intake of animal feed and drinking fluids was monitored so it did not differ between the control and experimental groups.

2.5.3. Feed or pellet composition and cholesterol fat enriched diet (CFED) production

Normal Pellets. Pellets from Rat Bio® by PT Citra Ina Feedmill have a composition consisting of 12% moisture content, 20% protein, 4% fat, 14% calcium fiber 1%, phosphorus 0.7%, total ash 11.5%, vitamin C: 0.3% and vitamin E 0.1%. It is recommended to store it in a cool and dry place to avoid direct sunlight.

CFED Production. The CFED diet was prepared according to previous work (de Oliveira et al., 2011). To Traditional mouse diet (dry pellets) was added. cholic acid (1%), cholesterol powder (2%), animal fat (20%, and 2% of corn oil (2%). Distilled water (1 L) was put in the mixer after hominization of the materials, and the pellets were then molded into smaller bits. The pellets were dried at standard room temperature under sterile circumstances before being conserved at 4 °C to minimize CFED oxidation. Carbohydrates make up 43.57 percent of CFED while protein makes up 12.38 percent, fiber makes up 4.73 percent, fat makes up 3.17 percent, cholesterol makes up 2 percent, cholic acid makes up 1 percent, animal fat makes up 20 percent, total ash makes up 4 percent, maize oil makes up 2 percent, and moisture makes up 6.85 percent.

2.5.4. Biomedical analysis of collected blood samples

After six weeks of mice interventional feeding, the blood sample was extracted. Preparation included mice fasting the night before blood was drawn with ketamine used as anesthesia. The venous sinus was the chosen location to draw blood, the collected blood was then put in a sterile and dry tube with no anticoagulant and was let to coagulate at room temperature. Then, centrifugation (3,000 rpm, 20 min) was done to obtain the serum. Biomedical analysis (LDL, triglyceride, HDL, total cholesterol, and blood glucose) was performed utilizing the COBAS Integra® 400 plus analyzer (Roche). Blood was also taken from liver tissue through the hepatic portal vein to evaluate superoxide dismutase (SOD) enzyme activities according to the product kit (superoxide dismutase assay kit Sigma-Aldrich). PGC-1α levels were calculated using Sunlong Biotech Co., Ltd.'s PGC-1α Mouse ELISA Kit to quantify PGC-1α concentration from liver tissue. TNF-α levels were calculated using the Mouse Tumor Necrosis Factor α (TNFα) Kit from liver tissue. Interleukin 10 (IL-10) levels were calculated using Abcam's IL-10 ELISA Kit from liver tissue. Serum lipase levels of mice were measured using Mouse Lipase, Pancreatic (PL) ELISA Kit. The body weights of mice were measured using digital scales.

2.6. Gut microbiota community analysis

2.6.1. DNA extraction and sequencing library generation

Stool samples were stored at −80 °C before microbiome gut analysis was performed. The statistical analysis allowed the researchers to select feces from the CFED only (B; Negative Control) and KBPF (D; High Dose) groups for gut microbiome analysis.

E.Z.N.A. ®Soil DNA Kit (Omega Bio-Tek, Norcross, GA, USA) was used to extract DNA from collected feces samples according to the listed protocol. A fluorometer (QuantiFluor™-ST, Promega Corporation, USA) was used to determine DNA quality. 466bp DNA fragments and region amplification and production were done utilizing paired primers in the V3–V4 region of 16s rDNA. The reverse primer used was 806R (-5-GGACTACHVGGGTATCTAAT-3-) with the forward primer of 341F (-5-CCTACGGGNGGCWGCAG-3-). Each PCR contains 2.5 µL of 10 × PCR buffer, 1 µL of each primer, 2 µL of dNTPs, and 20–30 ng of template DNA, with a total volume of 25 µL. After that, the generation of sequencing libraries was done by attaching the end of amplicons to the indexed adapters. Finally, QuantiFluor™ fluorometer was used to validate the libraries with the quantification to 10 nmol.

2.6.2. 16s rRNA gene sequencing and microbial community analysis

The operational taxonomic units (OTUs) were gathered using an Uparse software with standard clustering of 97% similarity. Paired-end data (2x250 bp) was collected using the Illumina platform (Illumina MiSeq). OTUs alignment with Greengene database Release 13.5 and species annotation was done utilizing the naive Bayesian assignment algorithm of the RDP classifier. Furthermore, Shannon, Chao1, and Simpson indices were used to determine gut microbiota alpha diversity. In contrast, principal coordinate analysis (PCoA) of Bray–Curtis dissimilarities was used to analyze the beta diversity. The disparities between groups were observed using linear discriminant effect size (LEfSe) analysis.

2.7. Data analysis and management

GraphPad Prism was utilized to perform the statistical analysis. *In vitro* data, Inhibition of ABTS, and enzymes (lipase, α-amylase, and α-glucosidase performed trice were statistically analyzed using an unpaired *t*-test. EC_{50} data were each derived from nonlinear regression equations. Meanwhile, in vivo set of data from each category (PGC-1α, LDL, HDL, TG, Blood glucose, SOD liver level, serum lipase, serum amylase, Total Cholesterol, IL-10, TNFα, and PGC-1α) were analyzed using multivariate ANOVA. Paired t-tests or dependent t-tests were performed to find significant differences between the initial and the final body weights (g) in each group. Furthermore, one-way ANOVA was performed to determine the significant differences between each secondary parameter (water intake (mL), food intake (g), food efficiency ratio (FER, %); initial, final, and daily weight gain (g/day)) of each group. The confidence level of all data was set a 95% and they are presented in the form of a Mean ± SEM. All in vitro and in vivo analysis uses GraphPad Prism version 9 software on MacBook devices. Visualization of 11 images and graphical abstracts using licensed Biorender Premium.

3. Results

3.1. Metabolites profile of KBPF

The peaks or ions of compounds present in kombucha butterfly pea flower (KBPF), their relative abundances and elution times from the LC-MS analysis are displayed in Fig. 1. Discovered compounds were automatically identified via mzCloud MS/MS Library (Thermo Scientific Q Exactive Software. Based on non-targeted metabolomic profiling A total of 79 molecules were successfully identified in KBPF (Fig. 1) and Table 2. The identification combined the electrospray ionization with Fourier transformation to yield spectra that can be matched to those in the database (Fig. 1A). Fig. 1B is an illustration where an electrospray positive weak peak 1.80 x 10ˆ6 counts is transform into a useable spectrum (*m/z* 50–750 Da). Details of the identified compounds based on non-targeted metabolomic profiling results with LC-HRMS with calculated molecular weight, molecular formula, and retention time are
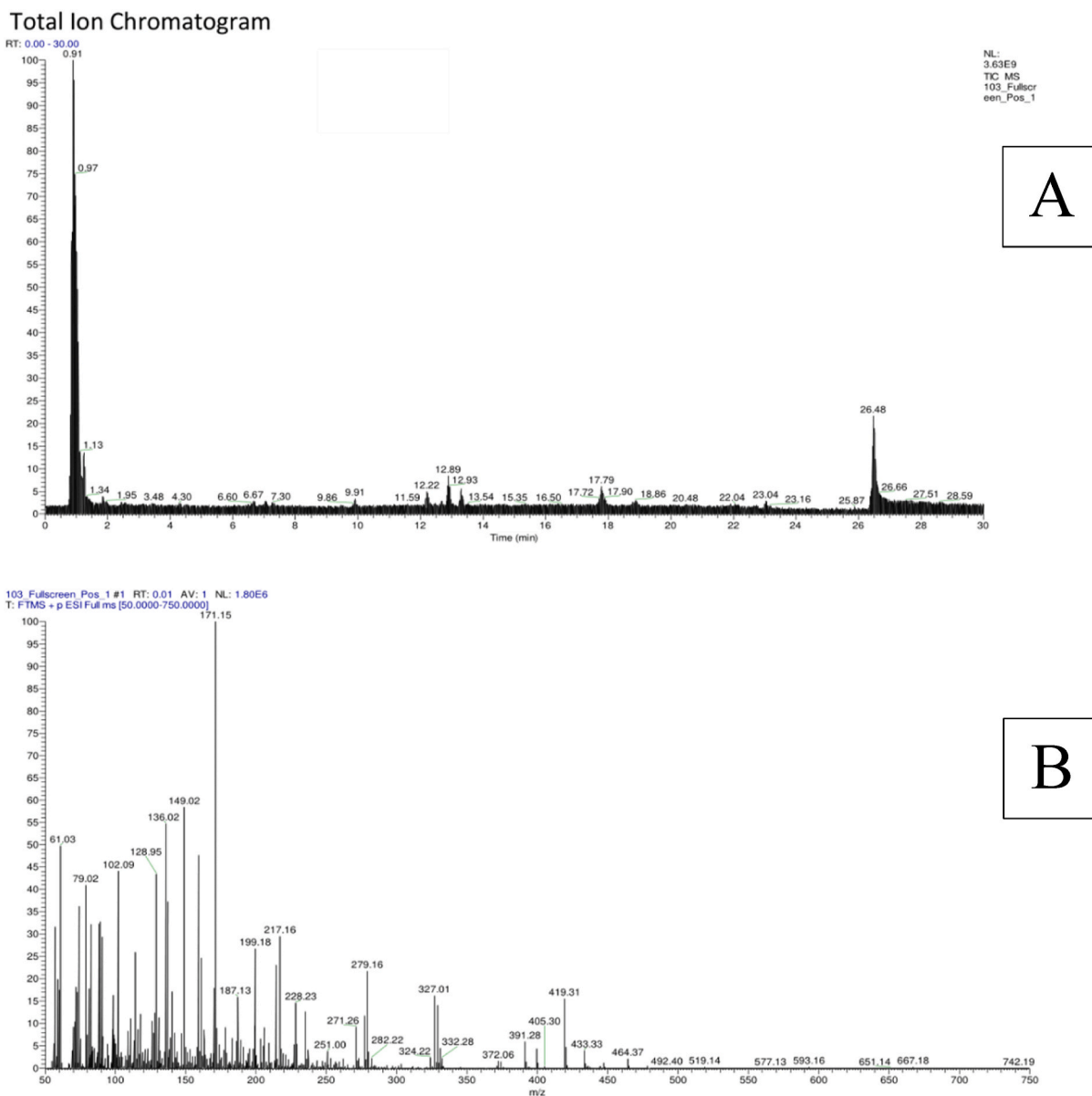
Fig. 1. Total Ion Chromatogram LC-MS of Kombucha Butterfly Pea Flower. Total ion chromatogram (ESI +) and the LC-MS metabolite profiles of KBPF (Fig. 1A). Positive ion mass spectra (FTMS-ESI (+)) of the m/z range 50–750 of KBPF (Fig. 1B).

S#: number of scans; RT: Retention time; AV: Averaged number of scans; SB: Subtracted (followed by subtraction information); NL: Neutral loss; T: Scan type; F: Scan filter.

presented in Table 2, sorted by their abundance.

3.2. In vitro studies

3.2.1. Lipase inhibition activity of KBPF
Inhibitory data of KBPF and the control orlistat are shown in Fig. 2. Orlistat exhibited a more potent lipase-inhibition activity than KBPF at all tested doses (Fig. 2A). EC$_{50}$ values of orlistat and KBPF in this study were 133.0 and 123.2 μg/mL, respectively (Fig. 2B). This result may be attributed to unequal maximum and baseline effect of KBPF compared to orlistat. For further research, using a lower minimum dose of orlistat/control and a higher maximum quantity of KBPF may result in comparable dose-response of both compounds (EC$_{50}$).

3.2.2. α-Glucosidase inhibition activity of KBPF
The results of the inhibition of α-glucosidase the control acarbose and the KBPF drink are shown in Fig. 3. Acarbose exhibited more potent

α-glucosidase-inhibition activity than KBPF at all doses (Fig. 3A). EC$_{50}$ values of acarbose and KBPF were 162.6 and 153.8 μg/mL, respectively (Fig. 3B). This result may be attributed to the unequal maximum and baseline effect of KBPF compared to acarbose in this study. For further research, using a lower minimum quantity of acarbose/control and a higher maximum quantity of KBPF may result in comparable dose-response of both compounds (EC$_{50}$).

3.2.3. α-Amylase inhibition activity of KBPF
The α-amylase inhibitory data are shown in Fig. 4. Acarbose showed greater inhibition of α-amylase activity than KBPF at 150 and 200 μg/mL doses (Fig. 4A). Meanwhile, at 50, 100, and 250 μg/mL there was no significant difference between KBPF and acarbose. EC$_{50}$ values of acarbose and KBPF were 162.6 and 160.2 μg/mL, respectively (Fig. 4B).

3.2.4. ABTS radical scavenging activity of KBPF
Fig. 5 depicts the ABTS radical scavenging activity of KBPF. These

Table 2
LC-HRMS analysis of Kombucha Butterfly Pea Flower (KBPF).

Tentatively Identified Compound	Molecular Formula	Calculated Exact Mass	RT (Min.)	Abundance (Area Max.)
2-[3-methyl-2-(methylimino)-4-oxo-1,3-thiazolan-5-yl]acetic acid	$C_7H_{10}N_2O_3S$	202.04442	0.904	10,839,195,649.98
5-({[3-chloro-5-(trifluoromethyl)-2-pyridyl]methyl}thio)-4-pentyl-4H-1,2,4-triazol-3-ol	$C_{14}H_{16}ClF_3N_4OS$	380.07048	0.956	5,991,074,606.21
D-(+)-Maltose	$C_{12}H_{22}O_{11}$	342.09673	0.929	5,845,139,637.52
Choline	$C_5H_{13}NO$	103.09952	1.037	769,699,623.67
Diisobutylphthalate	$C_{16}H_{22}O_4$	278.15074	17.786	617,534,658.14
5-Hydroxymethyl-2-furaldehyde	$C_6H_6O_3$	126.03132	0.899	501,292,279.09
2,2,6,6-Tetramethyl-1-piperidinol (TEMPO)	$C_9H_{19}NO$	157.14601	12.233	495,705,793.85
6-Gingerol	$C_{17}H_{26}O_4$	294.17151	12.899	427,316,447.04
Trigonelline	$C_7H_7NO_2$	137.02053	0.973	275,584,467.90
NP-004917	$C_{15}H_{26}O_3$	276.1715	13.309	257,509,864.99
1-Naphthol	$C_{10}H_8O$	144.05687	12.9	244,672,148.93
D-(+)-Proline	$C_5H_9NO_2$	115.063	0.976	225,662,810.91
Bis(2-ethylhexyl) phthalate	$C_{24}H_{38}O_4$	390.27538	23.042	221,505,943.89
11-piperidino-2,3-dihydro-1H-cyclopenta[4,5]pyrido[1,2-a]benzimidazole-4-carbonitrile	$C_{20}H_{20}N_4$	316.16396	12.898	146,810,705.72
4-Methoxybenzaldehyde	$C_8H_8O_2$	136.0519	12.899	146,599,833.81
Dibenzylamine	$C_{14}H_{15}N$	197.11975	7.286	139,615,759.44
L-Pyroglutamic acid	$C_5H_7NO_3$	129.04207	0.969	119,196,130.35
NP-001596	$C_{16}H_{30}O_4$	308.1953	18.861	114,561,846.60
L-Phenylalanine	$C_9H_{11}NO_2$	165.07843	1.862	110,692,221.82
(1S,4aS,7aS)-7-({[(2E)-3-phenylprop-2-enoyl]oxy}methyl)-1-{[(2S,3R,4S,5S,6R)-3,4,5-trihydroxy-6-(hydroxymethyl)oxan-2-yl]oxy}-1H,4aH,5H,7aH-cyclopenta[c]pyran-4-carboxylic acid	$C_{25}H_{28}O_{11}$	504.12334	0.863	106,748,469.46
L-Norleucine	$C_6H_{13}NO_2$	131.09419	1.369	89,557,756.62
DL-Stachydrine	$C_7H_{13}NO_2$	143.094	0.986	89,321,851.72
D-Raffinose	$C_{18}H_{32}O_{16}$	504.14952	0.846	88,220,518.35
DL-Arginine	$C_6H_{14}N_4O_2$	174.11102	1.016	85,708,926.51
3-{[(2S,3R,4S,5R,6R)-3,5-dihydroxy-6-(hydroxymethyl)-4-{[(2S,3R,4R,5R,6S)-3,4,5-trihydroxy-6-methyloxan-2-yl]oxy}oxan-2-yl]oxy}-5,7-dihydroxy-2-(4-hydroxyphenyl)-4H-chromen-4-one	$C_{27}H_{30}O_{15}$	594.15709	7.066	78,313,635.73
trans-3-Indoleacrylic acid	$C_{11}H_9NO_2$	187.06271	3.466	76,089,476.68
Adenine	$C_5H_5N_5$	135.05403	1.257	69,763,886.35
Eucalyptol	$C_{10}H_{18}O$	154.12473	6.692	63,991,259.52
Maltotriose	$C_{18}H_{32}O_{16}$	504.16769	1.152	59,422,862.80
Kaempferol	$C_{15}H_{10}O_6$	286.04653	7.066	59,418,932.46
D-Lactose monohydrate	$C_{12}H_{22}O_{11}$	360.11509	1.119	55,835,015.17
1,4:3,6-Dianhydro-2,5-dideoxy-2-[(ethylcarbamoyl)amino]-5-{[4-(3-fluorophenyl)-2-pyrimidinyl]amino}-L-iditol	$C_{19}H_{22}FN_5O_3$	387.17287	0.817	48,465,960.32
NP-013538	$C_{12}H_{16}O_8$	288.08348	1.142	48,071,291.82
L-Histidine	$C_6H_9N_3O_2$	155.06882	0.978	46,235,660.11
Zearalenone	$C_7H_{13}NO_2$	318.13255	17.922	45,690,501.48
Adenosine	$C_{10}H_{13}N_5O_4$	267.09593	1.259	43,089,483.64
α-Lactose	$C_{12}H_{22}O_{11}$	342.11508	0.835	42,515,962.32
3-(3,4-dihydroxyphenyl)propanoic acid	$C_9H_{10}O_4$	182.04682	1.276	40,328,477.06
Bis(3,5,5-trimethylhexyl) phthalate	$C_{26}H_{42}O_4$	418.27538	2.502	39,189,919.74
2′-Deoxyadenosine	$C_{10}H_{13}N_5O_3$	251.09952	0.971	37,766,344.25
L-Glutamic acid	$C_5H_9NO_4$	147.05264	0.901	37,332,424.63
Trifolin	$C_{21}H_{20}O_{11}$	448.09941	7.067	33,967,256.93
L(−)-Pipecolinic acid	$C_6H_{11}NO_2$	129.07862	1.252	33,105,793.50
Tributyl phosphate	$C_{12}H_{27}O_4P$	266.1639	16.373	31,854,835.20
Guanine	$C_5H_5N_5O$	151.04904	1.254	31,728,726.77
7-Hydroxycoumarine	$C_9H_6O_3$	162.03115	14.68	31,380,276.69
Citral	C10H16O	152.11962	6.493	30,955,705.46
L-Valine	$C_5H_{11}NO_2$	117.07863	1.253	27,634,464.41
methyl 2-(6-hydroxy-3-oxo-3H-xanthen-9-yl)benzoate	$C_{21}H_{14}O_5$	346.08647	0.895	26,511,069.86
Mauritianin	$C_{33}H_{40}O_{19}$	772.21465	6.648	26,277,739.75
Caprolactam	$C_6H_{11}NO$	113.08384	3.456	25,592,983.21
3,5-di-tert-Butyl-4-hydroxybenzaldehyde	$C_{15}H_{22}O_2$	234.16133	16.807	23,011,599.18
DEET	$C_{12}H_{17}NO$	191.13039	11.6	22,528,611.45
Rutin	$C_{27}H_{30}O_{16}$	610.15184	6.622	21,407,269.73
n-Pentyl isopentyl phthalate	$C_{18}H_{26}O_4$	306.20854	17.788	21,360,397.05
4-(2,3-dihydro-1,4-benzodioxin-6-yl)butanoic acid	$C_{12}H_{14}O_4$	222.07053	13.006	19,883,017.13
Luvangetin	$C_{15}H_{14}O_4$	258.08608	14.678	19,362,093.99
Tetranor-12(S)-HETE	$C_{16}H_{26}O_3$	266.17694	16.821	19,251,205.23
Crotonic acid	$C_4H_6O_2$	86.03686	1.259	16,735,205.90
4-{4-[3-(4-chlorophenoxy)propyl]piperazino}-1H-indole	$C_{21}H_{24}ClN_3O$	369.1624	1.175	16,573,523.70
Avobenzone	$C_{20}H_{22}O_3$	310.13783	12.9	13,530,322.90
3,5-di-tert-Butyl-4-hydroxybenzoic acid	$C_{15}H_{22}O_3$	250.15611	14.79	12,754,443.84
Quercetin	$C_{15}H_{10}O_7$	302.04167	6.621	11,681,843.04
NP-019988	$C_{10}H_{10}O_4$	176.04688	9.712	11,393,067.22
α-Pyrrolidinopropiophenone	$C_{13}H_{17}NO$	203.13054	16.478	11,202,837.62
NP-020014	$C_{15}H_{26}O_3$	276.1715	17.34	10,810,032.65
Acetylcholine	$C_7H_{15}NO_2$	145.10977	1.255	10,646,937.37
N-Cyclohexyl-N-methylcyclohexanamine	$C_{13}H_{25}N$	195.19815	7.206	10,324,790.92
2-Hydroxycinnamic acid	$C_9H_8O_3$	164.03627	4.607	9,786,462.42
Hexamethylenetetramine	$C_6H_{12}N_4$	140.10568	26.423	9,497,108.70

(continued on next page)

Table 2 (*continued*)

Tentatively Identified Compound	Molecular Formula	Calculated Exact Mass	RT (Min.)	Abundance (Area Max.)
N,N-Diisopropylethylamine (DIPEA)	$C_8H_{19}N$	129.15135	4.59	9,450,544.54
Nicotinamide	$C_6H_6N_2O$	122.04774	1.251	9,205,270.16
NP-008952	$C_{12}H_{20}O_4$	210.125	12.098	8,881,602.79
Vanillin	C8H8O3	152.04683	6.064	7,823,301.28
7,9-dimethoxy-6-(4-methoxyphenyl)-2H,8H-[1,3]dioxolo[4,5-g]chromen-8-one	$C_{19}H_{16}O_7$	356.08611	9.468	7,603,167.52
Quercetin-3β-D-glucoside	$C_{21}H_{20}O_{12}$	464.0941	7.098	7,129,490.50
Jasmonic acid	$C_{12}H_{18}O_3$	210.12251	6.492	6,134,146.60
L-(+)-Citrulline	$C_6H_{13}N_3O_3$	175.15033	4.306	6,111,632.66
Sunitinib	$C_{22}H_{27}FN_4O_2$	398.19594	6.068	5,609,740.58

RT = retention time (minutes).
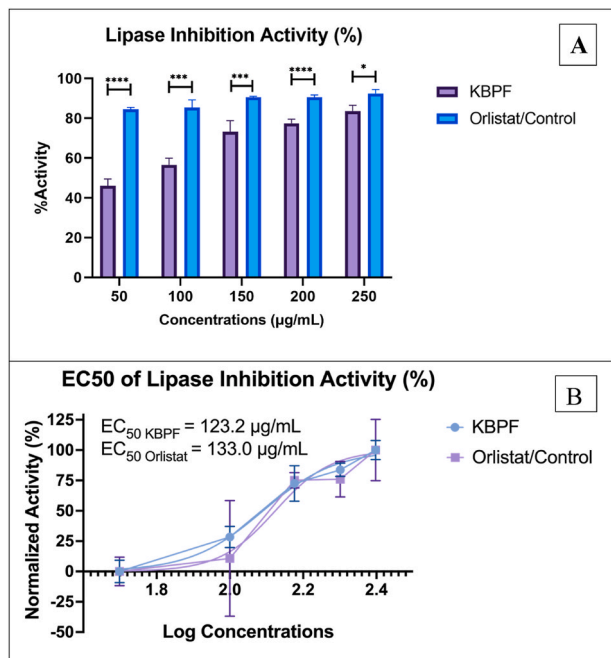
Fig. 2. Lipase Inhibition Activity Test of KBPF and Orlistat. The inhibition of lipase was presented in % activity (Fig. 2A) and EC_{50} value (Fig. 2B). ****$p = 0.0001$ and * = $p = 0.01$.

Fig. 3. α-Glucosidase Inhibition Activity Test of KBPF and Acarbose. The inhibition of α-glucosidase was presented in % activity (Fig. 3A) and EC_{50} value (Fig. 3B). ****$p = 0.0001$.

results show antioxidant activity that proves KBPF's capability to scavenge ABTS radical cations. The efficacy of ABTS radical scavenging activity from KBPF showed a dose-dependent curve, ranging from a percentage of activity of $65.07 \pm 4.30\%$ at 50 µg/mL and increased to $86.23 \pm 0.90\%$ at a concentration of 250 µg/mL (Fig. 5A). KBPF ABTS radical scavenging activity EC_{50} value was 156.1 µg/mL compared to 135.6 µg/ml for Trolox a standard antioxidant compound (Fig. 5B).

3.3. In vivo studies

Data on mice's body weight, weight gain (g/day), feed and water consumption, and feed efficiency ratio (FER) are presented in Table 3. The CON-NEG or B group (fed only CFED feed) had a final weight of 54.47 ± 4.38 g and a daily weight increased by 0.83 ± 0.13 g/day. The administration of CFED only (B) resulted in a significantly higher final body weight value for mice compared to other groups ($p < 0.0001$). However, the average daily weight gain (g/day) between the mice groups was not different ($p = 0.9899$). Additionally, the final body weights of groups A, C, and D were not different ($p > 0.05$) (Table 3). These results showed that the addition of the fermented drink to a cholesterol-enriched high-fat diet prevented the increase in body weight in groups C and D relatively to group B by maintaining normal body weight. When compared to the other groups, FER was considerably

greater in the CFED group (16.56 4.40%) ($p = 0.0025$). There were no appreciable differences in the groups' intake of food or liquids ($p = 0.9939$ and $p = 0.7869$, respectively).

3.3.1. Lipid profile and blood glucose

Lipid profile data including HDL, LDL, Triglycerides (TG), Total Cholesterol, and Blood Glucose data are presented in Fig. 6. High-density lipoprotein (HDL) levels were lowered significantly than the control group when mice were on the CFED diet ($p = 0.0001$). In contrast, when the CFED diet was supplemented with KBPF, HDL remained higher ($p < 0.05$). The effect of KBPF 130 mg/kg BW was more efficient than providing KBPF 65 mg/kg BW in increasing the HDL level of mice relative to CFED.

Fig. 6 also showed that low-density lipoprotein (LDL) increased significantly in mice that were given a CFED diet ($p = 0.0001$). LDL decreased or was considerably lower ($p < 0.05$), both in the control group and the treatment groups CFED + KBPF (65 mg/kg and 130 mg/kg BW). The effect of 130 mg/kg BW KBPF was more effective in reducing LDL.

Triglyceride (TG) levels were also considerably higher in the control group when mice were given a CFED diet, significantly ($p < 0.0001$). TG decreased or was considerably lower ($p < 0.05$), both in the control group and the treatment group when given CFED + KBPF 65 and 130
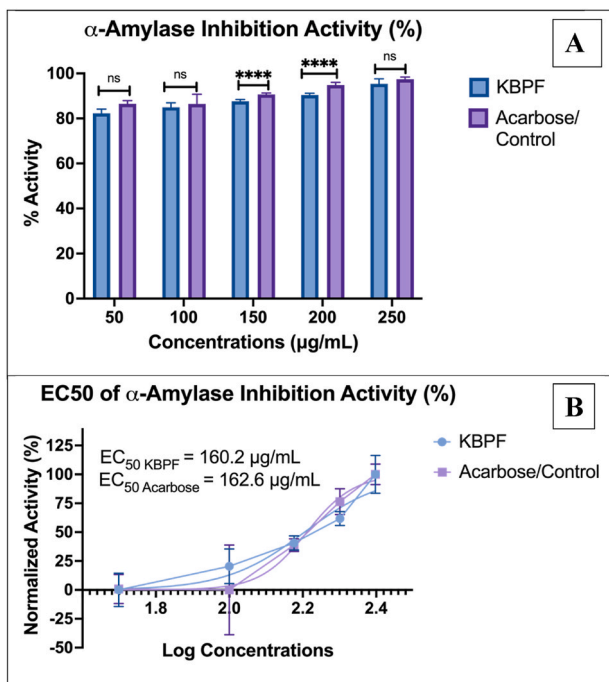
Fig. 4. α-Amylase Inhibition Activity Test of KBPF and Acarbose. The inhibition of α-glucosidase was presented in % activity (Fig. 4A) and EC$_{50}$ value (Fig. 4B). ****p = 0.0001 and ns = p > 0.05.
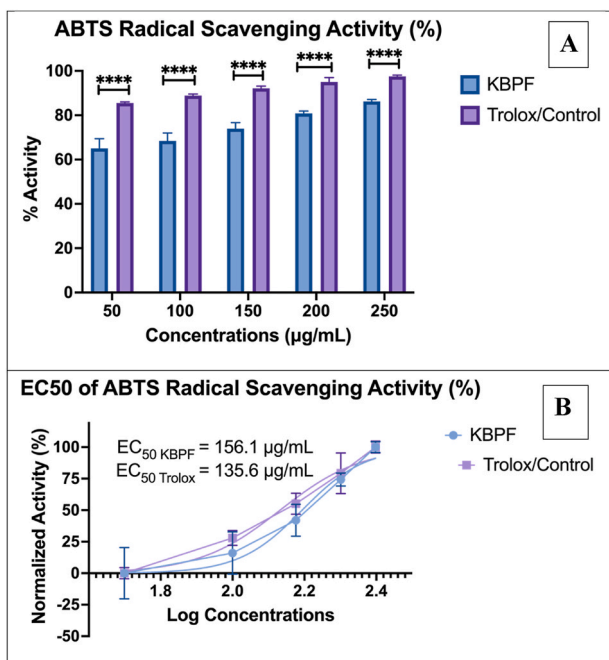
Fig. 5. ABTS Inhibition Activity Test of KBPF and Trolox. The inhibition of α-glucosidase was presented in % activity (Fig. 5A) and EC$_{50}$ value (Fig. 5B). ****p = 0.0001.

mg/kg with 130 mg/kg BW dose having a greater reduction.

In addition, Fig. 6 also showed that total cholesterol and fasting blood glucose increased significantly in mice fed the CFED diet compared to the control group (p = 0.0001). Total cholesterol and fasting blood glucose were significantly lower in both the control and experimental groups when given CFED + treatment of both doses of KBPF (p < 0.05). The effect of KBPF administration at low doses or 65

Table 3
Characteristics of body weight, feed and drinking intake, and FER of experimental mice.

Groups	A	B	C	D	p-value[b]
Initial Body Weight (g)	21.91 ± 1.35	21.15 ± 1.77	21.20 ± 1.69	21.86 ± 2.76	**0.8832**
Final Body Weight (g)	44.63 ± 2.04[a]	54.47 ± 4.38	44.20 ± 1.55[a]	45.26 ± 2.23[a]	**<0.0001**
p-value[a]	*<0.0001*	*<0.0001*	*<0.0001*	*<0.0001*	
Weight Gain (g/day)	0.57 ± 0.04	0.83 ± 0.13	0.58 ± 0.06	0.59 ± 0.10	**0.9899**
Food Intake (g)	4.98 ± 0.75	5.19 ± 0.81	4.84 ± 0.96	5.06 ± 0.91	**0.9939**
Water Intake (mL)	5.75 ± 0.70	5.60 ± 0.97	4.95 ± 0.76	5.09 ± 0.54	**0.7869**
FER (%)[1]	11.69 ± 2.21[a]	16.56 ± 4.40	12.14 ± 2.01[a]	11.93 ± 3.07[a]	**0.0025**

Percentage (%) of Food Efficiency Ratio or FER = (Body weight gain of mice (g/day)/food intake (g/day)) × 100.
[a] Dependent or Paired T-test CI 95% (0.05).
[b] MANOVA (Multivariate ANOVA) CI 95% (0.05). The letter (a) behind the number in the same row signifies no significant results.
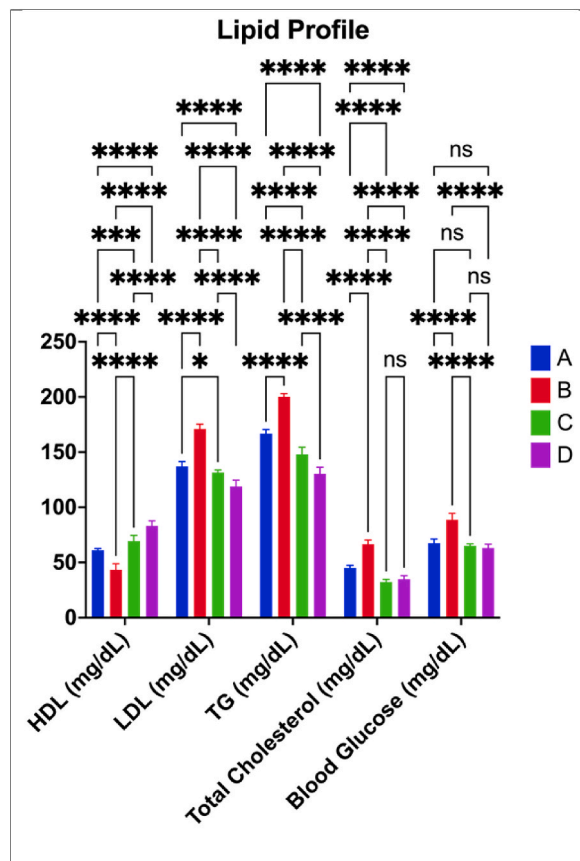
Fig. 6. Lipid Profile Improvement in Mice Given KBPF. *p = 0.01; ****p < 0.0001; ns → p > 0.05 (p = 0.4925). A = Control/Normal Diet; B = CFED Only; C = CFED + KBPF 65 mg/kg BW; D = CFED + KBPF 130 mg/kg BW.

mg/kg BW was more efficient than the administration of KBPF 130 mg/kg BW in lowering the total cholesterol of mice, b it was not significant (p > 0.05). Similar to total cholesterol, both doses of KBPF (65 and 130 mg/kg BW) had a similar hypoglycemic effect in the mice.

3.3.2. In vivo enzymatic assays

Data for the activity of the antioxidant enzyme, lipid hydrolyzing enzyme, superoxide dismutase (SOD) in the liver, lipase, and sugar hydrolyzing enzyme α-amylase in serum are presented in Fig. 7. The CFED diet significantly lowered the SOD liver activities compared to the control group (p < 0.0001). The inclusion of KBPF (65 and 130 mg/kg BW) into the CFED diet increased by 6 to 8-fold the SOD activity (p < 0.0001). In a similar trend to ABTS, HDL, and LDL, KBPF at 130 mg/kg BW was significantly more effective than giving KBPF at 65 mg/kg BW in increasing superoxide dismutase (SOD) liver activities (p < 0.0001).

The serum lipase and amylase activities as with other enzymes and markers were significantly altered (p < 0.0001 and 0.0002, respectively) when mice were given the CFED diet relative to those on the control diet. The addition of 65 and 130 mg KBPF/kg BW to the CFED diet + KBPF significantly lowered (p < 0.05) the activity of both enzymes. There were no significant differences between the two doses in reducing lipase activity (p = 0.1613). However, for α-amylase, the reduction of the 130 mg KBPF/kg BW was significant (p = 0.0160) relative to the 65 mg/kg dose. These results are aligned and supported by the in vitro test of lipase inhibition and α-amylase in Figs. 2 and 4. That KBPF in vitro and in vivo is shown to have potential lipase and α-amylase inhibitory activity.

3.3.3. Improved inflammatory molecular biomarkers by KBPF

The excess body mass is associated with inflammation and KBPF in mice had better effects on the tested biomarkers (PGC-1α, TNF-α, and interleukin (IL) 10) as shown in Fig. 8. PGC-1 α and IL-10 levels showed significantly higher value (p < 0.0001) in the treatment group (CFED + KBPF) as well as the control group. Including KBPF 65 mg/kg BW in the diet was more effective (p = 0.0238) than providing KBPF 130 mg/kg BW in increasing PGC-1α the level of the mice. However, for IL-10, the higher KBPF concentration resulted in better IL-10 levels (p = 0.0072)

Fig. 7. Improvements of Liver SOD, Lipase and Amylase Serum Activity in Mice Given KBPF. *p = 0.0160; ***p = 0.0002; ****p < 0.0001; ns → p > 0.05 (p = 0.1613). A = Control/Normal Diet; B = CFED Only; C = CFED + KBPF 65 mg/kg BW; D = CFED + KBPF 130 mg/kg BW.
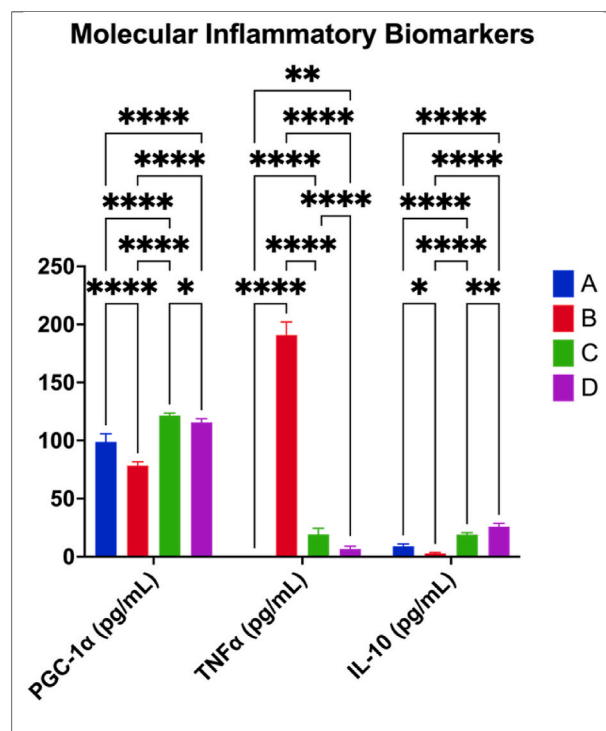
Fig. 8. Improvement of Inflammatory Biomarkers Activity on Mice Given KBPF. *p = 0.0238; **p = 0.0072; ****p < 0.0001. A = Control/Normal Diet; B = CFED Only; C = CFED + KBPF 65 mg/kg BW; D = CFED + KBPF 130 mg/kg BW. TNFα in control groups was not observed.

than the lower one. The CFED diet alone induced a significant increase in TNF-α levels (p < 0.0001) which was countered by the inclusion of KBPF in the diet. The dose of 130 mg KBPF/kg BW has the greatest reduction.

3.3.4. Gut microbiome altering by KBPF

Firmicutes were the predominant bacteria in CFED mice at the phylum level, followed by *Bacteroidetes*. After administration of kombucha into the CFED diet of the mice, the *Bacteroidetes* phylum was statistically higher (p = 0.01), and the *Firmicutes* phylum was statistically lower (p = 0.001) in the mice feces. At the genus level, *Lactobacillus*, *Morganella*, *Clostridium*, *Blautia*, and *Bacteroides* were the predominant genera that comprised the gut microbiota in both groups. Among these genera, the relative abundance of *Lactobacillus* and *Bacteroides* were significantly different (p = 0.004 and p = 0.01, respectively) between the CFED and high dose of the KBPF group. The *Lactobacillus* genus was higher in CFED mice, while the *Bacteroides* genus was higher in the high dose KBPF group (Fig. 9a).

The alpha and beta diversity of the gut microbiota was also analyzed. Mice supplemented with KBPF has higher alpha diversity indices (Shannon, Simpson, and Chao1 indexes) compared with a high fat-high cholesterol-fed diet, although statistically not significant (p > 0.05) (Fig. 9b). This result indicated that KBPF supplementation could increase the gut microbiota diversity in cholesterol- and fat-enriched diets (CFED). Although the alpha diversity was not statistically significant, the gut microbiota composition between CFED and KBPF groups was significantly different according to PERMANOVA analysis (p = 0.001). The principal coordinates analysis (PCoA) was performed, and the PCoA plot showed a clear separation between the two groups, indicating dissimilarity of the gut microbiota composition among groups (Fig. 9c). To analyze bacterial composition that differed between CFED and KBPF supplementation, LEfSe comparison was used (Fig. 9d). The results indicated that *Lactobacillus* and *Coprococcus* were significantly enriched in the CFED group with LDA score >3.5 while the rest have an LDA score
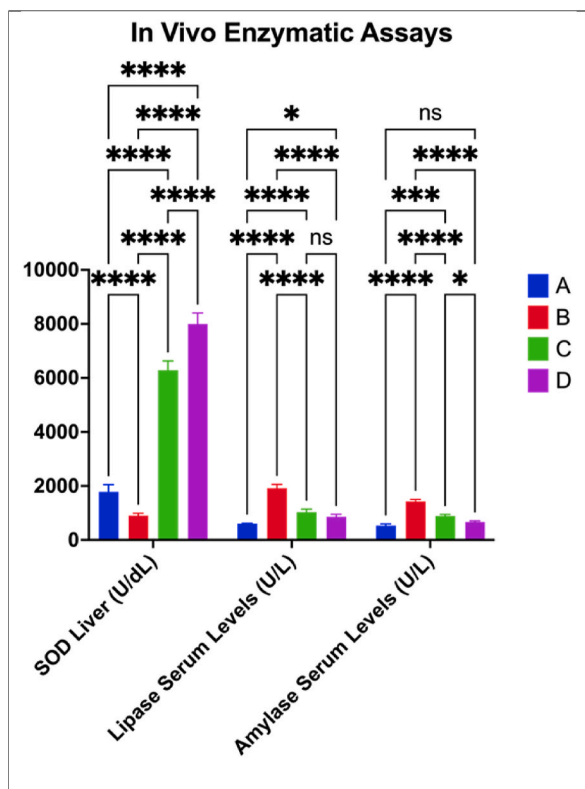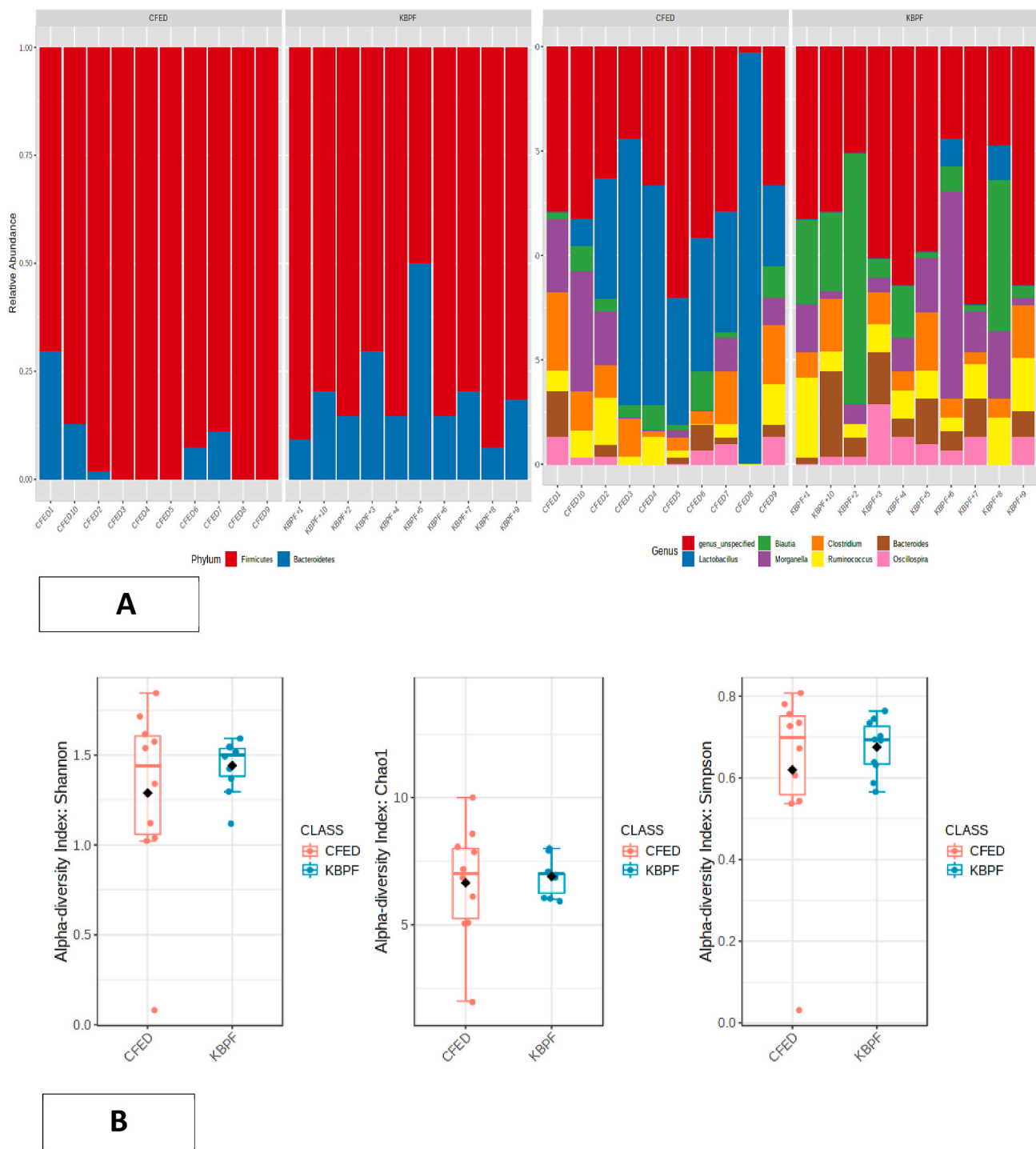
Fig. 9. Microbiome composition of mice supplemented with High-dose of KBPF. (9A) Bar plots visualize relative abundances of phylum and genera. Each bar represents a mice sample, and each color represents a phylum or genera. (9B) Using class data, alpha diversity was measured using Shannon, Chao1, and Simpson indexes. (9C) Principal coordinates analysis (PCoA) or beta diversity based on Bray-Curtis dissimilarity using the relative abundance of the genus. (9D) LEfSe analysis identified the most differently abundant genus among groups. (9E) Heatmap Pearson correlation analysis between several gut microbiota with certain metabolic and inflammatory biomarkers. (For interpretation of the references to color in this figure legend, the reader is referred to the Web version of this article.)

of <3.5. However, the gut microbiota of mice supplemented with KBPF significantly have higher enrichment in *Blautia, Bacteroides, Parabacteroides, Pharscolarctobacterium,* and *Proteus* with LDA score >3.5 (Fig. 9d). Pearson correlation analysis showed that there was significant correlation between several gut microbiota with certain metabolic profiles (Fig. 9E). Serum of blood glucose, total cholesterol, triglyceride,

LDL, TNF-α, lipase, and amylase have significant negative correlation with family of *Ruminococcaceae, Enterobacteriaceae*, and *Lachnospiraceae*. Serum HDL, IL-10 and PGC-1α have significant negative correlation with family of *Lactobacillaceae, Clostridiaceae*, and *Coriobacteriaceae*.
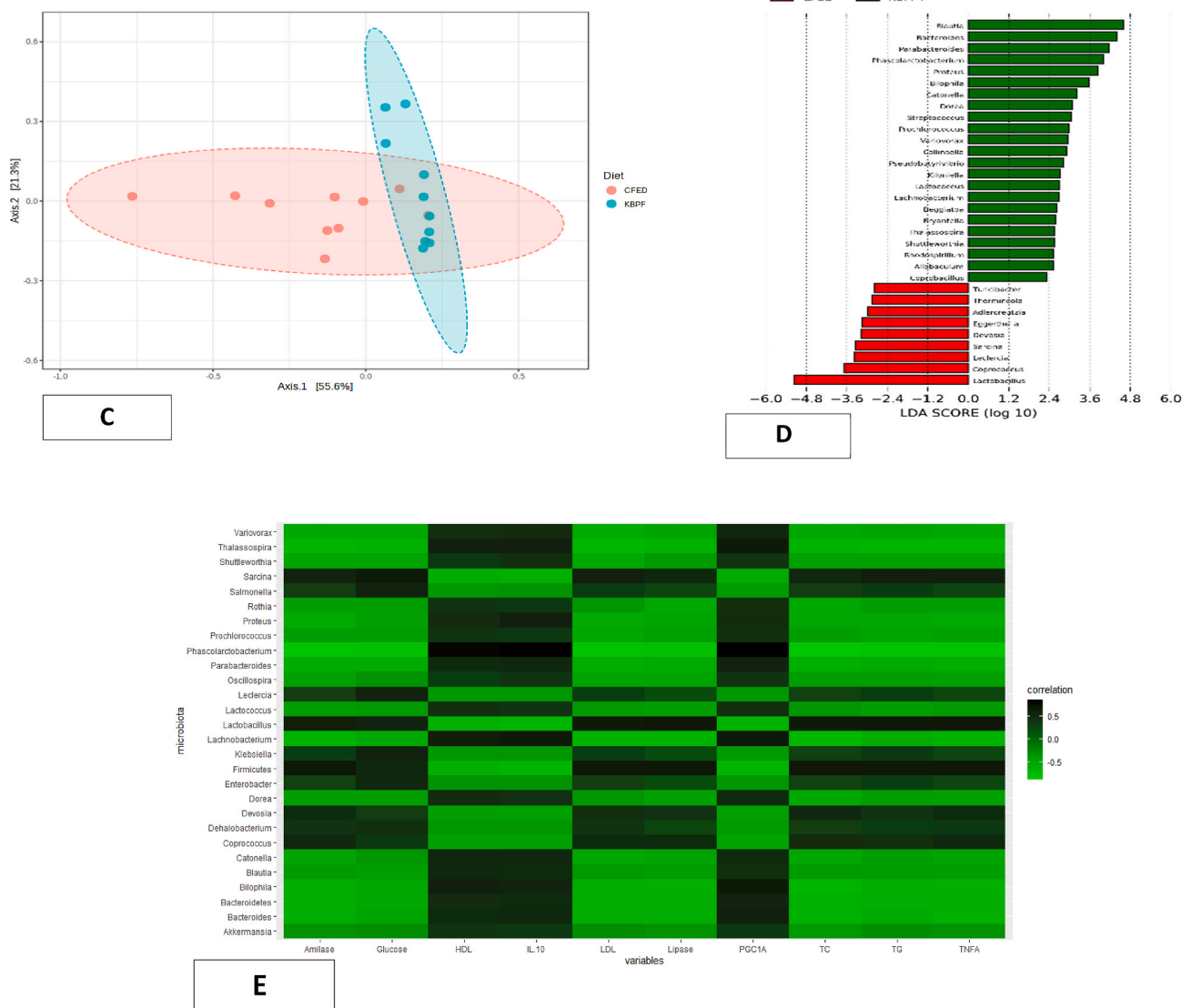
Fig. 9. (*continued*).

4. Discussions

There have been many utilizations of *Clitoria ternatea* or Butterfly pea, a herbal or medicinal plant in part because it is a good source of antioxidants (Oguis et al., 2019). Seeing the potential of the Butterfly pea, this work incorporated the butterfly pean into an innovative kombucha probiotic drink and evaluated its activity in vitro and in a mice model under a cholesterol high fat-enriched diet. The work successfully identified 79 secondary metabolites in the new kombucha dring (i.e. KBPF) (Table 2 and Fig. 1) many of which likely contributed to the biological function of the drink. These results showed the fermented drink contained far more metabolites (about 4-fold) from the Butterfly pea compared to 19 metabolites reported from the butterfly pea in the absence of fermentation (Lijon et al., 2017). This is in line with other studies that show that the fermentation process, especially using the kombucha or SCOBY technique, can increase bioactive compounds in a food product (Permatasari et al., 2021, 2022a; Augusta et al., 2021; Tanner et al., 2022). Although the metabolites identified in this work likely contributed to the biological activity of the new kombucha drink, future research should explore the use of bioinformatics, computational modeling, or in silico molecular dockings to determine the biological significance of the discovered butterfly pea metabolites.

In vitro, this work demonstrated the antioxidant (ABTS radical scavenging activity), inhibition of lipase, α-glucosidase, and α-amylase properties of the KBPF drink. These properties are important to mitigate or prevent metabolic disorders. KBPF has an EC_{50} in ABTS radical scavenging activity value of 156.1 µg/mL (Fig. 5) while butterfly pea flower without fermentation has been reported to have EC_{50} of 1 mg/mL and 4 mg/mL by other researchers (Iamsaard et al., 2014). This antioxidant activity is thought to be derived from several Polyphenolic compounds identified in KBPF such as kaempferol, rutin, and quercetin are well known for their radical scavenging properties and other biofunctions (Nurkolis et al., 2020) and may have contributed to the obtained data. In addition, the inhibition of lipase, α-amylase, and α-glucosidase obtained from KBPF showed their potential as functional food products. On a weight basis, KBPF at doses of 50, 100, and 250 µg/mL in vitro enzyme inhibitions were similar to acarbose, a control that inhibits α-amylase in diabetic patients (Rosak and Mertes, 2012).

An animal model was further used to assess the multi-functional properties of KBPF. Data showed that its inclusion in a high cholesterol-enriched high-fat diet improved lipid profile followed by the maintained inflammatory biomarkers such as PGC-1α, TNFα, and IL-10 at concentrations close to those found in mice that received a normal diet. In line with the in vitro results, the antioxidant status of mice

treated with KBPF was enhanced as illustrated by the increased activity of the superoxide dismutase (SOD) enzyme in the liver. Higher activity of the liver SOD will prevent oxidation and can therefore explain the better lipid profile and better regulation of inflammatory biomarkers in mice that received CFED + KBPF control to those that were on CEFD diet only. improvements. In most cases, as expected KBPF, at 130 mg/kg BW has a better effect. Superoxide dismutase (SOD) has an essential role as a defence mechanism against stress from oxidation in the human body (Younus, 2018). This enzyme acts as an excellent therapeutic agent against diseases mediated by reactive oxygen species (ROS), such as metabolic disorders and inflammation (Younus, 2018; Mohammadi et al., 2017; Montano et al., 2012). The latest systematic review and meta-analysis study reported that the consumption of antioxidants that also increase SOD levels has succeeded in suppressing inflammation by free radicals and metabolic disorders (Farhangi and Mohammad-Rezaei, 2021).

Carbohydrate intake and metabolism play significant roles in the development of metabolic disorders. Oligosaccharides that enter the gastrointestinal tract, predominantly after food intake, are hydrolyzed into maltose and maltotriose by a key enzyme named α-amylase (Gong et al., 2020). Pancreatic and salivary α-Amylase act as catalyzers to the hydrolysis reaction of α-1,4-glucan linkages, creating smaller disaccharides (Yang et al., 2019). Furthermore, α-Glucosidase, another carbohydrate found on the surface of intestinal mucose cells, continues the process by cleaving disaccharides' linkages and releasing absorbable monosaccharides that are transported into the circulation (Patil et al., 2015; Zaklos-Szyda et al., 2015). Results from this showed that KBPF successfully inhibited both carbohydrates (α-Amylase, α-Glucosidase), subsequently prolonging carbohydrate digestion duration, which will then lower postprandial glucose and hyperglycemia if present (Patil et al., 2015). This mechanism mimics alpha-glucosidase inhibitors, utilized as anti-diabetic drugs, like acarbose and voglibose. Hence KBPF

presents a promising alternative remedial strategy for managing hyperglycemia (Fig. 10).

Meanwhile, in lipid metabolism, lipid ingested in the form of triglycerides is converted to monoglycerides and fatty acids by pancreatic, lingual, and gastric lipase. Together with cholesterol and bile acid, the lipid products form mixed micelles that diffuse across intestinal cell membranes. Inside these cells, triglycerides are formed back and combined with apolipoproteins to form chylomicrons inside the Golgi apparatus to be circulated into the blood (Liu et al., 2020; Chandwad and Gutte, 2019). Chylomicrons will spread across body tissues, accumulating mainly in adipose tissues. In excess lipid intake conditions, over-accumulation of triglycerides in the liver causes adverse alterations of chylomicrons regulation and lipolysis, as well as cholesterol-ester exchange, amplifying increase of LDL, TG, body weight, and decreasing HDL levels (Klop et al., 2013) (Fig. 10). High carbohydrate and fat diets can also trigger de novo lipogenesis, converting abundant carbohydrates into fatty acids, which are then converted to triacylglycerols through esterification (Klop et al., 2013). The obtained data showed that KBPF could substantially inhibit lipase enzymes, therefore impairing excess lipid metabolism, improving lipid profiles including LDL, triglyceride, and body weight reduction, and increasing HDL (Fig. 10).

The development of metabolic disorders and their complications are strongly associated with inflammation and oxidative stress. Adipocyte hypertrophy caused by constant energy surplus provokes the release of adipokines in the form of pro-inflammatory cytokines such as interleukin-10 (IL-10) and tumor necrosis factor-alpha (TNF-α), causing low-grade inflammation (Ameer et al., 2014). Hyperglycemia, excess lipid, and chronic low-grade inflammation can cause different reactive oxygen species (ROS) production, producing oxidant/antioxidant imbalance, hence oxidative stress, which results in excessive activation of NADPH oxidase. This process will lead to the generation of superoxide
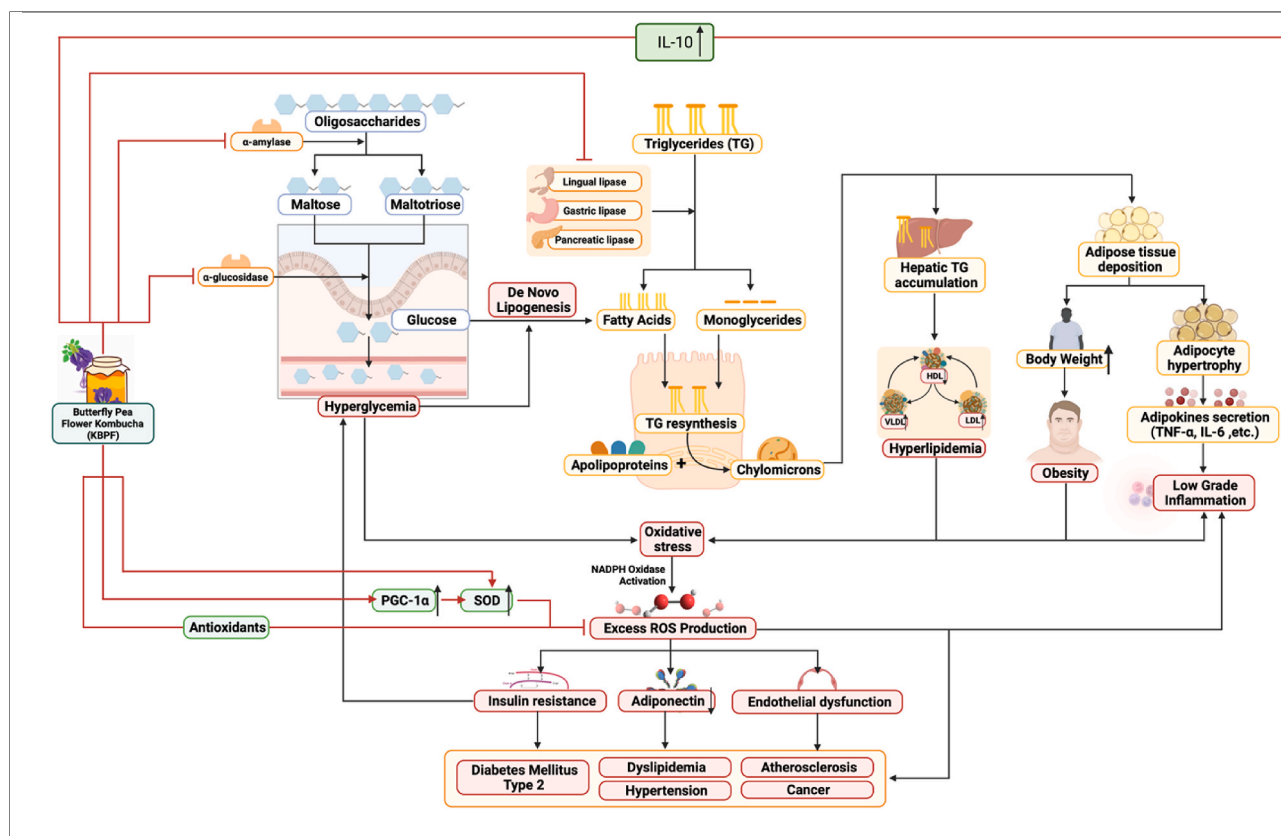
Fig. 10. Mechanism of Butterfly pea flower kombucha in alleviating metabolic syndrome with immunomodulatory effect. Abbreviations can be found in the abbreviation list section above or in the page title.

anion, the main ROS (Francisqueti et al., 2017). Consequently, increased ROS can decrease adiponectin, further inflammation, endothelial dysfunction, and insulin resistance. Further progression of this condition will cause hypertension, dyslipidemia, diabetes type 2, atherosclerosis, and even cancer (Araújo et al., 2022). Results from this study showed that KBPF intake could suppress ROS levels (ABTS, SOD data) as well as decrease major inflammatory cytokines (TNF-α, IL-6) significantly, potentially preventing the emergence and progression of metabolic disorders in its consumers (Fig. 10).

As seen in this study, the elevation of PGC-1α levels by KBPF administration might contribute to the antioxidative potential. PGC-1α is a master transcriptional coactivator for mitochondrial biogenesis and cell respiration. Recent studies have shown PGC-1α as a key player in modulating the expression of ROS-eliminating enzymes (Luca et al., 2019). Studies have shown patients with metabolic syndrome have increased circulatory oxidative stress biomarkers and decreased anti-oxidant levels, such as vitamin C and superoxide dismutase (SOD) (Matsuda and Shimomura, 2013; Kang and Ji, 2013). Other than the previous findings, this study showed that KBPF high-dose administration also increased SOD serum markedly. SOD is one of the effective anti-oxidant defenses that have an indispensable role in neutralizing free-radical excess (Austin and St-Pierre, 2012). SOD can catalyze the transformation of superoxide anion into hydrogen peroxide and molecular oxygen, in which hydrogen peroxide is then further broken down by catalase into water and oxygen molecules (Austin and St-Pierre, 2012; Zelzer et al., 2011; Spahis et al., 2017; Ighodaro and Akinloye, 2018; Rosa et al., 2021). The increase in PGC-1α activity mentioned above is assumed to play a part in alleviating SOD levels (McMeekin et al., 2021).

In addition, high-dose KBPF supplementation or mice in group D (CFED + KBPF 130 mg/kg BW) has been observed to provide abundant gut microbiota diversity compared to group B or CFED only (Fig. 9). he gut microbiota provides an essential role in the ethiology of metabolic syndrome, as confirmed by studies conducted on both human and animal in vivo models (Festi et al., 2014). Abundant microbiome gut diversity is also associated with lipid profile improvement and reducing the risk of inflammation (Festi et al., 2014; Wang et al., 2020; Sanz et al., 2010). As the dominant genus of the gut microbiota, *Blautia* found abundantly in the KBPF group plays a particular role in metabolic diseases, inflammatory diseases, and biotransformation (Sohail et al., 2019). However, in the Liu et al. (2021) study, most of the properties of this genus are related to the function of potential probiotics, and the causal relationship between *Blautia* abundance and disease is not yet clear (Liu et al., 2021). This study found a significant positive correlation between *Blautia* and HDL, IL-10, PGC-1α (Fig. 9E). Furthermore, the serum of blood glucose, total cholesterol, triglyceride, LDL, TNF-α, lipase, and amylase have negative correlation with *Blautia*. This research supports the latest reference regarding the benefits of *Blautia* abundance in metabolic disorders and inflammatory diseases. The diversity of *Bacteroides* and *Parabacteroides* was also abundant in mice's feces, given high doses of KBPF supplementation. *Bacteroides* and *Parabacteroides* are potential probiotics for the therapeutics of systemic and intestinal inflammatory diseases, such as inflammatory bowel disease (IBD). The results of this study support previous research by Hiippala et al., 2020) (Hiippala et al., 2020). More interestingly, *Pharscolarctobacterium* diversity is also found in feces that are given high doses of KBPF supplementation. *Phascolarctobacterium* is an essential probiotic manufacturer of acetic acid and propionic acid and has been reported to have a positive correlation with the mood in humans (Wu et al., 2017). Seeing its potential in increasing the diversity of *Phascolarctobacterium*, KBPF is also possible as a psychobiotic agent, but further clinical research is needed in the future. Overall, KBPF supplementation of 130 mg/kg BW also alters or modulates the diversity of the gut microbiome important in fighting metabolic syndrome and inflammatory diseases.

In general, KBPF has promising potential as a prospective nutraceutical for patients with metabolic and inflammatory disorders,

including improving hyperglycemia in diabetic patients, suppressing hyperlipidemia, hypercholesterolemia, and weight loss in obese patients (Fig. 10). An increase in PGC-1α also contributes to a wide range of positive impacts on oxidative metabolism, which can benefit patients with metabolic and inflammatory disorders (Fig. 10). However, some limitations make this study less likely to be that this study is a preclinical trial or in vivo test that certainly does not represent the results in humans. Therefore, it is hoped that there will be further clinical trial research in humans to support the clinical mechanism of the health benefits of butterfly pea flower kombucha (KBPF). In addition, researchers realized that due to limited research funding, gut microbiome analysis was only carried out in selected groups, namely the CFED-only group (B) and the high-dose KBPF group (D), which had previously been mentioned in the method section. In addition, levels of Fatty Acids, especially SCFA (Short Chain Fatty Acid), and intake of dietary fibers were not seen as parameters in this study due to the limited research funds available. In addition, the dosage results of these preclinical trials can be used as a reference in human clinical trials in the future. It is also hoped that the data from exploring KBPF metabolite compounds can be tested in silico so that they know their potential as therapeutics for other diseases.

5. Conclusions

Clitoria ternatea or Butterfly pea flower can be processed or innovated into a functional probiotic drink, namely KBPF, which has 79 potential secondary metabolite compounds. Butterfly pea flower kombucha (KBPF) exhibits promising antioxidant, anti-metabolic disorders, and anti-inflammatory activity in alleviating metabolic disorders and inflammatory diseases in vitro and in vivo. Followed by a good modulation of gut microbiome diversity, KBPF can be a promising therapeutic functional food in preventing metabolic syndrome with an immuno-modulatory effect.

Data availability statement

The data displayed in this study are available via sending a request to the corresponding author with approval or can be found in the supplementary 1.

Availability of data and material

Data is available by requesting an application through email to the corresponding author.

CRediT authorship contribution statement

Happy Kurnia Permatasari: conduct experiments, analyzed data, write the manuscript, design research, and conceptualize ideas. **Fahrul Nurkolis:** conduct experiments, analyzed data, write the manuscript, design research, and conceptualize ideas. **William Ben Gunawan:** contribute to data analysis, critiquing manuscript, interpreting manuscript results, assisting in the data processing, as well as revising and editing the graphical abstract, critiquing, reviewing, writing & revising the manuscript. All authors have read and also accepted this final manuscript. **Vincentius Mario Yusuf:** contribute to data analysis, critiquing manuscript, interpreting manuscript results, assisting in the data processing, as well as revising and editing the graphical abstract. **Muhammad Yusuf:** contribute to data analysis, critiquing manuscript, interpreting manuscript results, assisting in the data processing, as well as revising and editing the graphical abstract. **Rio Jati Kusuma:** contribute to data analysis, critiquing manuscript, interpreting

manuscript results, assisting in the data processing, as well as revising and editing the graphical abstract. **Nindy Sabrina:** critiquing, reviewing, writing & revising the manuscript. All authors have read and also accepted this final manuscript. **Farizal Rizky Muharram:** critiquing, reviewing, writing & revising the manuscript. All authors have read and also . **Nurpudji Astuti Taslim:** critiquing, reviewing, writing & revising the manuscript. All authors have read and also . **Nelly Mayulu:** critiquing, reviewing, writing & revising the manuscript. All authors have read and also . **Siti Chairiyah Batubara:** critiquing, reviewing, writing & revising the manuscript. All authors have read and also . **Mrinal Samtiya:** critiquing, reviewing, writing & revising the manuscript. All authors have read and also accepted this final manuscript. **Hardinsyah Hardinsyah:** critiquing, reviewing, writing & revising the manuscript, All authors have read and also accepted this final manuscript. **Apollinaire Tsopmo:** final manuscript, final manuscript, final manuscript, final manuscript, critiquing, reviewing, writing & revising the manuscript, All authors have read and also accepted this final manuscript.

Declaration of competing interest

The authors declare that they have no known competing financial interests or personal relationships that could have appeared to influence the work reported in this paper.

Acknowledgments

Appendix A. Supplementary data

Supplementary data to this article can be found online at https://doi.org/10.1016/j.crfs.2022.08.005.

References

Ameer, F., Scandiuzzi, L., Hasnain, S., Kalbacher, H., Zaidi, N., 2014 Jul 1. De novo lipogenesis in health and disease. Metabolism 63 (7), 895–902. https://doi.org/10.1016/j.metabol.2014.04.003.

Araújo, M.C., Soczek, S.H., Pontes, J.P., Marques, L.A., Santos, G.S., Simão, G., Bueno, L. R., Maria-Ferreira, D., Muscará, M.N., Fernandes, E.S., 2022. An overview of the TRP-oxidative stress Axis in metabolic syndrome: insights for novel therapeutic approaches. Cells 11 (8), 1292. https://doi.org/10.3390/cells11081292.

Augusta, P.S., Nurkolis, F., Noor, S.L., Permatasari, H.K., Taslim, N.A., Batubara, S.C., Mayulu, N., Wewengkang, D.S., Rotinsulu, H., 2021. Probiotic beverage: the potential of anti-diabetes within kombucha tea made from sea grapes *(Ceulerpa racemosa)* containing high antioxidant and polyphenol total. Proc. Nutr. Soc. 80 (OCE3) https://doi.org/10.1017/S002966512100272X.

Austin, S., St-Pierre, J., 2012 Nov 1. PGC1α and mitochondrial metabolism—emerging concepts and relevance in ageing and neurodegenerative disorders. J. Cell Sci. 125 (21), 4963–4971. https://doi.org/10.1242/jcs.113662.

Chandwad, S.C., Gutte, S.L., 2019. Screening of actinomycetes for lipase inhibitors production. Int. J. Pharm. Biol. Sci. IJPBSTM 9 (3), 277–281. https://doi.org/10.21276/ijpbs.2019.9.3.39.

Chen, H., Zheng, X., Zong, X., Li, Z., Li, N., Hur, J., et al., 2021. Metabolic syndrome, metabolic comorbid conditions and risk of early-onset colorectal cancer. Gut 70, 1147–1154. https://doi.org/10.1136/gutjnl-2020-321661.

de Oliveira, J.C., Scomparin, D.X., Andreazzi, A.E., Branco, R.C., Martins, A.G., Gravena, C., Grassiolli, S., Rinaldi, W., Barbosa, F.B., Mathias, P.C., 2011 Feb. Metabolic imprinting by maternal protein malnourishment impairs vagal activity in adult rats. J. Neuroendocrinol. 23 (2), 148–157 doi: 10.1111/j.1365-2826.2010.02095.x. PMID: 21091554.

Farhangi, M.A., Mohammad-Rezaei, A., 2021. Higher dietary total antioxidant capacity (TAC) reduces the risk of cardio-metabolic risk factors among adults: an updated systematic review and meta-analysis. Int. J. Vitam. Nutr. Res. 1 (1), 1–15. https://doi.org/10.1024/0300-9831/a000708.

Festi, D., Schiumerini, R., Eusebi, L.H., Marasco, G., Taddia, M., Colecchia, A., 2014. Gut microbiota and metabolic syndrome. World J. Gastroenterol.: WJG 20 (43), 16079. https://doi.org/10.3748/wjg.v20.i43.16079.

Francisqueti, F.V., Chiaverini, L.C., Santos, K.C., Minatel, I.O., Ronchi, C.B., Ferron, A.J., Ferreira, A.L., Corrêa, C.R., 2017. The role of oxidative stress on the pathophysiology of metabolic syndrome. Rev. Assoc. Méd. Bras. 63, 85–91. https://doi.org/10.1590/1806-9282.63.01.85.

Gong, L., Feng, D., Wang, T., Ren, Y., Liu, Y., Wang, J., 2020 Dec. Inhibitors of α-amylase and α-glucosidase: potential linkage for whole cereal foods on prevention of hyperglycemia. Food Sci. Nutrition 8 (12), 6320–6337. https://doi.org/10.1002/fsn3.1987.

Grundy, S.M., 2016. Metabolic syndrome update. Trends Cardiovasc. Med. 26, 364–373. https://doi.org/10.1016/j.tcm.2015.10.004.

Hardy, D.S., Racette, S.B., Garvin, J.T., Gebrekristos, H.T., Mersha, T.B., 2021. Ancestry specific associations of a genetic risk score, dietary patterns and metabolic syndrome: a longitudinal ARIC study. BMC Med. Genom. 14, 118. https://doi.org/10.1186/s12920-021-00961-8.

Hiippala, K., Kainulainen, V., Suutarinen, M., Heini, T., Bowers, J.R., Jasso-Selles, D., Lemmer, D., Valentine, M., Barnes, R., Engelthaler, D.M., Satokari, R., 2020. Isolation of anti-inflammatory and epithelium reinforcing Bacteroides and Parabacteroides spp. from a healthy fecal donor. Nutrients 12 (4), 935. https://doi.org/10.3390/nu12040935.

Iamsaard, S., Burawat, J., Kanla, P., Arun, S., Sukhorum, W., Sripanidkulchai, B., Uabun-Dit, N., Wattathorn, J., Hipkaeo, W., Fongmoon, D., Kondo, H., 2014 Jun. Antioxidant activity and protective effect of Clitoria ternatea flower extract on testicular damage induced by ketoconazole in rats. J. Zhejiang Univ. - Sci. B. 15 (6), 548–555. https://doi.org/10.1631/jzus.B1300299.

Ighodaro, O.M., Akinloye, O.A., 2018. First line defence antioxidants-superoxide dismutase (SOD), catalase (CAT) and glutathione peroxidase (GPX): their fundamental role in the entire antioxidant defence grid. Alexandria J. Med. 54 (4), 287–293. https://doi.org/10.1016/j.ajme.2017.09.001.

Kang, C., Ji, L.L., 2013 Jun 1. Role of PGC-1α in muscle function and aging. J. Sport Health Sci. 2 (2), 81–86. https://doi.org/10.1016/j.jshs.2013.03.005.

Klop, B., Elte, J.W.F., Cabezas, M.C., 2013. Dyslipidemia in obesity: mechanisms and potential targets. Nutrients 5 (4), 1218–1240. https://doi.org/10.3390/nu5041218.

Lijon, M.B., Meghla, N.S., Jahedi, E., Rahman, M.A., Hossain, I., 2017 Jan. Phytochemistry and pharmacological activities of Clitoria ternatea. Int. J. Nat. Soc. Sci. 4 (1), 1, 0.

Liu, T.T., Liu, X.T., Chen, Q.X., Shi, Y., 2020 Aug 1. Lipase inhibitors for obesity: a review. Biomed. Pharmacother. 128, 110314 https://doi.org/10.1016/j.biopha.2020.110314.

Liu, X., Mao, B., Gu, J., Wu, J., Cui, S., Wang, G., Zhao, J., Zhang, H., Chen, W., 2021 Jan-Dec. Blautia-a new functional genus with potential probiotic properties? Gut Microb. 13 (1), 1–21. https://doi.org/10.1080/19490976.2021.1875796. PMID: 33525961; PMCID: PMC7872077.

Luca, M., Di Mauro, M., Perry, G., 2019 Jul 4. Neuropsychiatric disturbances and diabetes mellitus: the role of oxidative stress. Oxid. Med. Cell. Longev. 2019. https://doi.org/10.1155/2019/5698132.

Martini, N.K.A., Ekawati, N.G.A., Ina, P.T., 2020. Pengaruh suhu dan lama pengeringan terhadap karakteristik teh bunga telang (*Clitoria ternatea L.*). Jurnal Ilmu Dan Teknologi Pangan (ITEPA) 9 (3), 327–340. https://doi.org/10.24843/itepa.2020.v09.i03.p09.

Matsuda, M., Shimomura, I., 2013 Sep 1. Increased oxidative stress in obesity: implications for metabolic syndrome, diabetes, hypertension, dyslipidemia, atherosclerosis, and cancer. Obes. Res. Clin. Pract. 7 (5), e330–e341. https://doi.org/10.1016/j.orcp.2013.05.004.

McMeekin, L.J., Fox, S.N., Boas, S.M., Cowell, R.M., 2021 Feb 9. Dysregulation of PGC-1α-dependent transcriptional programs in neurological and developmental disorders: therapeutic challenges and opportunities. Cells 10 (2), 352. https://doi.org/10.3390/cells10020352. PMID: 33572179; PMCID: PMC7915819.

Mohammadi, E., Qujeq, D., Taheri, H., Hajian-Tilaki, K., 2017. Evaluation of serum trace element levels and superoxide dismutase activity in patients with inflammatory bowel disease: translating basic research into clinical application. Biol. Trace Elem. Res. 177 (2), 235–240. https://doi.org/10.1007/s12011-016-0891-0.

Montano, M.A.E., da Cruz, I.B.M., Duarte, M.M.M.F., da Costa Krewer, C., Mânica-Cattani, M.F., Soares, F.A.A., Rosa, G., Maris, A.F., Battiston, F.G., Trott, A., Lera, J. P.B., 2012. Inflammatory cytokines in vitro production are associated with Ala16Val superoxide dismutase gene polymorphism of peripheral blood mononuclear cells. Cytokine 60 (1), 30–33. https://doi.org/10.1016/j.cyto.2012.05.022.

Noce, A., Di Lauro, M., Di Daniele, F., Pietroboni Zaitseva, A., Marrone, G., Borboni, P., et al., 2021. Natural bioactive compounds useful in clinical management of metabolic syndrome. Nutrients 13, 630. https://doi.org/10.3390/nu13020630.

Nurkolis, F., Surbakti, F.H., Sabrina, N., Azni, I.N., Hardinsyah, H., 2020. Mango sugar rich in vitamin C: a potency for developing functional sugar rich in antioxidants. Curr. Develop. Nutr. 4 (Suppl. ment_2), 765. https://doi.org/10.1093/cdn/nzaa052_034, 765.

Oguis, G.K., Gilding, E.K., Jackson, M.A., Craik, D.J., 2019. Butterfly pea (*Clitoria ternatea*), a cyclotide-bearing plant with applications in agriculture and medicine. Front. Plant Sci. 10, 645. https://doi.org/10.3389/fpls.2019.00645.

Patil, P., Mandal, S., Tomar, S.K., Anand, S., 2015 Sep. Food protein-derived bioactive peptides in management of type 2 diabetes. Eur. J. Nutr. 54 (6), 863–880. https://doi.org/10.1007/s00394-015-0974-2.

Permatasari, H.K., Nurkolis, F., Augusta, P.S., Mayulu, N., Kuswari, M., Taslim, N.A., Wewengkang, D.S., Batubara, S.C., Gunawan, W.B., 2021. Kombucha tea from seagrapes *(Caulerpa racemosa)* potential as a functional anti-ageing food: in vitro and in vivo study. Heliyon 7 (9), e07944. https://doi.org/10.1016/j.heliyon.2022.e09348.

Permatasari, H.K., Firani, N.K., Prijadi, B., Irnandi, D.F., Riawan, W., Yusuf, M., Amar, N., Chandra, L.A., Yusuf, V.M., Subali, A.D., Nurkolis, F., 2022a. Kombucha drink enriched with sea grapes *(Caulerpa racemosa)* as potential functional beverage to contrast obesity: an in vivo and in vitro approach. Clin. Nutr. ESPEN. https://doi.org/10.1016/j.clnesp.2022.04.015.

Permatasari, H.K., Nurkolis, F., Hardinsyah, H., Taslim, N.A., Sabrina, N., Ibrahim, F.M., Visnu, J., Kumalawati, D.A., Febriana, S.A., Sudargo, T., Tanner, M.J., 2022b. Metabolomic assay, computational screening, and pharmacological evaluation of caulerpa racemosa as an anti-obesity with anti-aging by altering lipid profile and peroxisome proliferator-activated receptor-γ coactivator 1-α levels. Front. Nutr. 1412. https://doi.org/10.3389/fnut.2022.939073.

Rodrigues, Brian, Margaret, C Cam, Kong, Jian, Ramesh K, Goyal, John H, McNeill, April 1997. Strain differences in susceptibility to streptozotocin-induced diabetes: effects on hypertriglyceridemia and cardiomyopathy. Cardiovasc. Res. 34 (Issue 1), 199–205. https://doi.org/10.1016/S0008-6363(97)00045-X.

Rojas, M., Chávez-Castillo, M., Pirela, D., Parra, H., Nava, M., Chacín, M., et al., 2021. Metabolic Syndrome: is it time to add the central nervous system? Nutrients 13, 2254. https://doi.org/10.3390/nu13072254.

Rosa, A.C., Corsi, D., Cavi, N., Bruni, N., Dosio, F., 2021 Mar 25. Superoxide dismutase administration: a review of proposed human uses. Molecules 26 (7), 1844. https://doi.org/10.3390/molecules26071844.

Rosak, C., Mertes, G., 2012. Critical evaluation of the role of acarbose in the treatment of diabetes: patient considerations. Diabetes Metab. Syndr. Obes. 5, 357–367. https://doi.org/10.2147/DMSO.S28340. Epub 2012 Oct 12. PMID: 23093911; PMCID: PMC3476372.

Saklayen, M.G., 2018. The global epidemic of the metabolic syndrome. Curr. Hypertens. Rep. 20, 12. https://doi.org/10.1007/s11906-018-0812-z.

Sancho, L., Yahia, E., González-Aguilar, G., 2013. Contribution of major hydrophilic and lipophilic antioxidants from papaya fruit to total antioxidant capacity. Food Nutr. Sci. 4 (8A), 93–100. https://doi.org/10.4236/fns.2013.48A012.

Sanz, Y., Santacruz, A., Gauffin, P., 2010. Gut microbiota in obesity and metabolic disorders. Proc. Nutr. Soc. 69 (3), 434–441. https://doi.org/10.1017/S0029665110001813.

Sohail, M.U., Yassine, H.M., Sohail, A., Thani, A.A., 2019. Impact of physical exercise on the gut microbiome, inflammation, and the pathobiology of metabolic disorders. Rev. Diabet. Stud. 15 (1), 35–48. https://doi.org/10.1900/RDS.2019.15.35.

Spahis, S., Borys, J.M., Levy, E., 2017 Mar 20. Metabolic syndrome as a multifaceted risk factor for oxidative stress. Antioxidants Redox Signal. 26 (9), 445–461. https://doi.org/10.1089/ars.2016.6756.

Tanner, M.J., Nurkolis, F., Mayulu, N., Taslim, N.A., Achadi, E., Permatasari, H.K., Wewengkang, D.S., Hardinsyah, H., 2022. Sea grapes kombucha tea improves liver-superoxide dismutase (SOD) serum in mice fed on cholesterol-and fat-enriched diet: a novel probiotic ready-to-drink rich in ascorbic acid. Proc. Nutr. Soc. 81 (OCE2) https://doi.org/10.1017/S0029665122000891.

Torres, S., Fabersani, E., Marquez, A., Gauffin-Cano, P., 2019. Adipose tissue inflammation and metabolic syndrome. the proactive role of probiotics. Eur. J. Nutr. 58, 27–43. https://doi.org/10.1007/s00394-018-1790-2.

Torres, S., Verón, H., Contreras, L., Isla, M.I., 2020. An overview of plant-autochthonous microorganisms and fermented vegetable foods. Food Sci. Hum. Wellness 9, 112–123. https://doi.org/10.1016/j.fshw.2020.02.006.

van Namen, M., Prendergast, L., Peiris, C., 2019. Supervised lifestyle intervention for people with metabolic syndrome improves outcomes and reduces individual risk factors of metabolic syndrome: a systematic review and meta-analysis. Metabolism 101, 153988. https://doi.org/10.1016/j.metabol.2019.153988.

Wang, P.X., Deng, X.R., Zhang, C.H., Yuan, H.J., 2020. Gut microbiota and metabolic syndrome. Chin. Med. J. 133 (7), 808–816. https://doi.org/10.1097/CM9.0000000000000696.

Wu, F., Guo, X., Zhang, J., Zhang, M., Ou, Z., Peng, Y., 2017. Phascolarctobacterium faecium abundant colonization in the human gastrointestinal tract. Exp. Ther. Med. 14 (4), 3122–3126. https://doi.org/10.3892/etm.2017.4878.

Yang, C.Y., Yen, Y.Y., Hung, K.C., Hsu, S.W., Lan, S.J., Lin, H.C., 2019 Aug 27. Inhibitory effects of pu-erh tea on alpha glucosidase and alpha amylase: a systemic review. Nutr. Diabetes 9 (1), 1–6. https://doi.org/10.1038/s41387-019-0092-y.

Younus, H., 2018 May-Jun. Therapeutic potentials of superoxide dismutase. Int. J. Health Sci. 12 (3), 88–93. PMID: 29896077; PMCID: PMC5969776.

Zaklos-Szyda, M., Majewska, I., Redzynia, M., Koziolkiewicz, M., 2015 Dec 1. Antidiabetic effect of polyphenolic extracts from selected edible plants as α-amylase, α-glucosidase and PTP1B inhibitors, and β pancreatic cells cytoprotective agents-a comparative study. Curr. Top. Med. Chem. 15 (23), 2431–2444. https://doi.org/10.2174/1568026615666150619143051.

Zelzer, S., Fuchs, N., Almer, G., Raggam, R.B., Prüller, F., Truschnig-Wilders, M., Schnedl, W., Horejsi, R., Möller, R., Weghuber, D., Ille, R., 2011 Jul 15. High density lipoprotein cholesterol level is a robust predictor of lipid peroxidation irrespective of gender, age, obesity, and inflammatory or metabolic biomarkers. Clin. Chim. Acta 412 (15–16), 1345–1349. https://doi.org/10.1016/j.cca.2011.03.031.